GlcNAc. From these results and enzyme specificity, the structure of N13-1 is tentatively predicted to be Galβ1-4(Fucα1-3)HexNAc-Galβ1-3GlcNAcβ1-3Galβ1-4Glc. After the fucosyl residue of N13-1 was digested with α1,3/4-fucosidase, the defucosylated product was cleaved by endo-β-galactosidase. The products of the digestion showed two peaks by HPLC, corresponding Glc-PA and GlcNAcβ1-3Galβ1-4Glc-PA, indicating that the subterminal HexNAc is GlcNAc linked β1-3 to galactose. Hence, the structure of N13-1 is predicted to be Galβ1-4(Fucα1-3)GlcNAcβ1-3Galβ1-3GlcNAcβ1-3Galβ1-4Glc ($V^3Fuc\alpha\text{-}_{1,2}Lc_6$). Sialylated GSL A18 was digested with α2,3-sialidase in conditions in which this enzyme cleaves the terminal α2,6-linkage (see *Material and methods*). The digestion product ran on the 2D map at the same position as the defucosylated product of N13-1. The structure of A18 is thus predicted to be NeuAcα2-6Galβ1-4GlcNAcβ1-3Galβ1-3GlcNAcβ1-3Galβ1-4Glc ($VI^6NeuAc\alpha\text{-}_{1,2}Lc_6$).

Structure of monosulfated GSLs, A5, A6, A10-1, A13-2, A14, A15, A16-2, A17, A19, A20, and A21

A5, A6, A10-1 A14, A15, and A20 are nonsialylated but have a HSO_3–6GlcNAc structure at their subterminal or terminal GlcNAc, as evidenced below. Our preliminary experiments revealed that methanolysis under the conditions used in this study hydrolyzes about 90% of the sulfate-linked galactose or GlcNAc residues, 75% of fucosyl residues linked β1-3 or β1-4 to GlcNAc, and a small amount of GlcNAc-Gal linkages. Therefore, when sulfo-fucosylated oligosaccharide was treated by methanolysis, the desulfated-defucosylated product appeared as the main peak and various other peaks such as sulfo-defucosylated product and desulfated-fucosylated product appeared. A14 was methanolyzed and the products appeared at the position of Galβ1-4(Fucα1-3)GlcNAcβ1-3Galβ1-3GlcNAcβ1-3Galβ1-4Glc ($V^3Fuc\alpha\text{-}_{1,2}Lc_6$), Galβ1-4GlcNAcβ1-3Galβ1-3GlcNAcβ1-3Galβ1-4Glc ($_{1,2}Lc_6$), sulfated-nonfucosylated product coinciding with A10-1, and Lc_4 on the map (data not shown). The results of methanolysis suggested that A14 was a sulfated form of Galβ1-4(Fucα1-3)GlcNAcβ1-3Galβ1-3GlcNAcβ1-3Galβ1-4Glc. Digestion of A14 with α1,3/4-fucosidase resulted in conversion to A10-1, in agreement with the result of methanolysis (Figure 3). It has been reported that Jack bean β-galactosidase can hydrolyze Galβ1-4(HSO_3–6)GlcNAc, whereas β1–4 galactosidase from *Streptococcus pneumoniae* cannot hydrolyze the linkage. After defucosylation, A14 could be digested with Jack bean β-galactosidase, but not with β1-4 galactosidase from *S. pneumoniae,* and the position of the agalacto form is identical to A5 on the map (Figure 3). Digestion of the agalacto form with human placental β-*N*-acetylhexosaminidase, which is able to cleave terminal HSO_3–6GlcNAc residues, released a HexNAc-HSO_3 residue, as measured by mass spectrometry (data not shown), and the product of the digest coincided with the position of the reference compound Lc_4 (Figure 3). These results indicate that the sulfate residue of A14 is linked to the 6-position of a subterminal GlcNAc (Table IV).

The structures of A20 and A6 were predicted to be Galβ1-4(Fucα1-3)(HSO_3–6)GlcNAcβ1-3Galβ1-4(Fucα1-3)GlcNAcβ1-3Galβ1-4Glc and Galβ1-4(Fucα1-3)(HSO_3–6)GlcNAcβ1-3Galβ1-4Glc by combination of methanolysis, enzymatic digestion with α1,3/4-fucosidase, Jack bean β-galactosidase and β1-4 galactosidase from *S. pneumoniae,* and mass spectrometry analysis, as was performed in the analysis of A14 (Figure 3). After digestion with α1,3/4-fucosidase, A20 was converted to A15 (Figure 3).

A13-2, A16-2, A17, A19, and A21 are monosialylated, monosulfated GSLs. Sialic acid is linked α2-3 to the terminal residue of A16-2 and A21 and linked α2-6 to the terminal residue of A13-2 and A19 as determined by the specificity of α2,3-silalidase digestion as described in *Material and methods*. The digestion products of A13-2, A16-2, A19, and A21 corresponded to A10-1, A14, A15, and A20, respectively, on the map (Figure 3). Although A17 is also a monosialylated, monosulfated GSL, the sialic acid is not linked to terminal galactose. In contrast to A13-2, A16-2, A19, and A21, A17 could not be digested with α2,3-sialidase even in conditions where this enzyme cleaves both the α2-3 and α2-6 linkages to the terminal residue but could be digested with neuraminidase from *Arthrobacter ureafaciens* which cleaves sialic acid linked to internal residues as well as sialic acid α2-3 and α2-6 linked to the terminal residue. This result suggests that sialic acid is linked to an internal residue of A17. A17 could be digested with α1,3/4-fucosidase. After α1,3/4-fucosidase and neuraminidase digestion, A17 was converted to A10-1 (Figure 3). These results indicate that the structure of A17 is such that sialic acid is attached to an internal residue, probably an internal GlcNAc, of Galβ1-4(Fucα1-3)(HSO_3-6)GlcNAc-Galβ1-3GlcNAcβ1-3Galβ1-4Glc. To determine the position of sialylation, A17 was sequentially digested with α1,3/4-fucosidase, Jack bean β-galactosidase, and then human placental β-*N*-acetylhexosaminidase. The digestion product was identical to LST-b, Galβ1-3(NeuAcα2-6)GlcNAcβ1-3Galβ1-4Glc, as expected (Figure 3).

The structures of A5, A6, A10-1, A13-2, A14, A15, A16-2, A17, A19, A20, and A21 are presented in Table IV.

The structure of disialylated GSLs, A10-2, and A13-1

A10-2 and A13-1 are disialylated on a tetrasaccharide backbone (Table III). A10-2 was digested with α2,3-sialidase in conditions in which this enzyme specifically cleaves the α2-3 linkage (condition 1). The digestion product corresponded to LST-b, Galβ1-3(NeuAcα2-6)GlcNAcβ1-3Galβ1-4Glc (data not shown). The structure of A10-2 is predicted to be NeuAcα2-3Galβ1-3(NeuAcα2-6)GlcNAcβ1-3Galβ1-4Glc. Similarly, A13-1 was sequentially digested with α2,3-sialidase in condition 1, followed by α1,3/4-fucosidase. The digestion product was identical to LST-b. The structure of A13-1 is therefore predicted to be NeuAcα2-3Galβ1-3(NeuAcα2-6)(Fucα1-4)GlcNAcβ1-3Galβ1-4Glc.

The predicted structures of the acidic and neutral GSLs of CCs from case 1 are presented in Table IV.

Structures of GSLs of colon cancer cells and normal colon epithelial cells from case 2

Although a variety of unusual GSLs were found in the CCs from case1 as shown above, the profiles of GSLs from CCs and NCs from case 2 are very similar to those observed in the other patients reported in the recent paper and subsequent analyses, except that two sulfated GSLs are included in the acidic fraction as minor components. Hence, only the profiles of the acidic GSLs of CCs and NCs from case 2 are shown in Figure 4. Thirteen peaks (A1–A13) and nine peaks were obtained from the

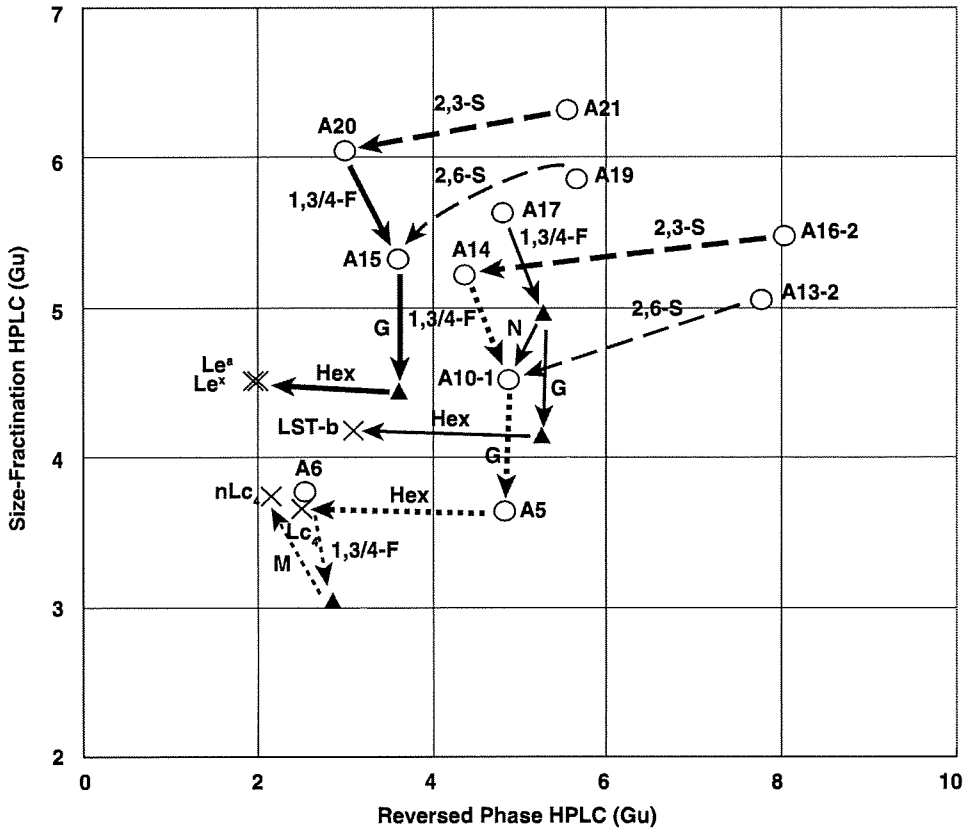

Fig. 3. Sequential digestion and methanolysis of PA-oligosaccharides, A5, A6, A10-1, A13-2, A14, A15, A16-2, A17, A19, A20, and A21. Circles indicate the positions of A5, A6, A10-1, A13-2, A14, A15, A16-2, A17, A19, A20, and A21. Thick-line, thin-line, thick dotted-line, and thin dotted-line arrows indicate the direction of the change after glycosidase digestion or methanolysis of A20, A17, A14, and A6, respectively. The thick broken line indicates the direction of the change after α2-3 sialidase digestions of A16-2 and A21 under conditions where the enzyme specifically digests sialic acid in the α2-3 linkage. The thin broken line indicates the direction of the change after α2-3 sialidase digestions of A13-2 and A19 under conditions where the enzyme digests sialic acid in both α2-3 and α2-6 linkages. The thin broken line from A19 to A15 is curved so as not to cross A17. Glycosidases are shown beside each line. Enzyme abbreviations are: 2,3-S; α2,3-sialidase under conditions where the enzyme specifically digests sialic acid in the α2-3 linkage, 2,6-S; α2,3-sialidase under conditions where the enzyme digests sialic acid in both α2–3 and α2-6 linkages, 1,3/4-F; α1,3/4-fucosidase, G; β-galactosidase from Jack bean, Hex; β-*N*-acetylhexosaminidase from human placenta, N; α-sialidase (neuraminidase) from *Arthrobacter ureafaciens*. M indicates methanolysis. X marks the positions of the standard compounds. Closed triangles mark the positions on the way in sequential enzymatic digestion.

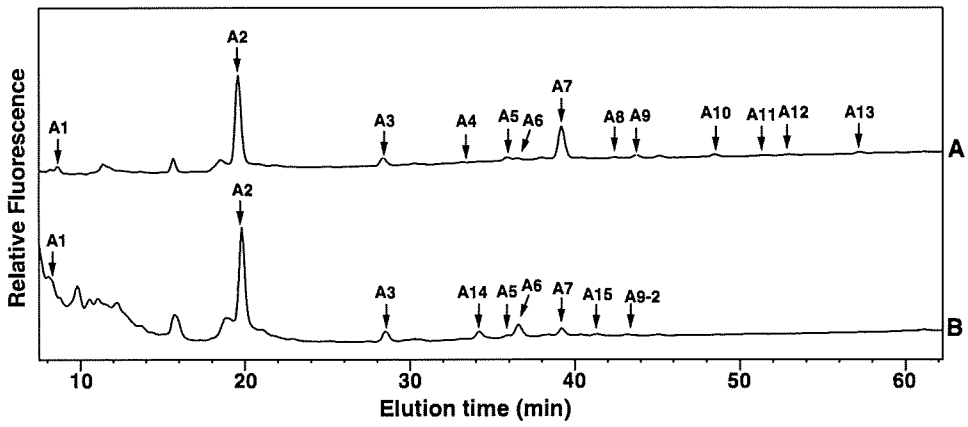

Fig. 4. Size fractionation HPLC of acidic PA-oligosaccharide mixtures obtained from CCs and NCs from case 2. (**A**) acidic fraction of CCs and (**B**) acidic fraction of NCs. Thirteen major peaks found in acidic fractions of CCs are represented as A1-A13 and highlighted with arrows (**A**). Nine major peaks found in acidic fractions from NCs are numbered as per the peak numbers of CCs (**B**). A14 and A15 in NCs, which were not observed in CCs, are GM1 and GD1b, respectively.

acidic GSLs of the CCs and NCs, respectively (Figure 4). Each of these peaks was further purified by reversed-phase HPLC. Peaks A8, A9, and A11 in CCs were separated by reversed-phase HPLC into two major components and designated A8-1, A8-2, A9-1, A9-2, A11-1, and A11-2. All nine peaks from NCs were separated by reversed-phase HPLC into single components. Additionally, purified PA-oligosaccharides were subjected to LC/ESI MS/MS. From a comparison of the positions

Table IV. Estimated structures of acidic and neutral PA-oligosaccharides from colon cancer cells of case 1

Fraction	Structure	Abbreviation	Ratio (%)
Acidic			
A1	HSO_3-3Galβ1-4Glc-PA	SM3	6.9
A2	Neu5Acα2-3Galβ1-4Glc-PA	GM3	3.3
A3	HSO_3-3Galβ1-3GlcNAcβ1-3Galβ1-4Glc-PA	3′-Sulfo-Lc_4	0.2
A4	Neu5Acα2-8Neu5Acα2-3Galβ1-4Glc-PA	GD3	0.2
A5	HSO_3 (6) GlcNAcβ1-3Galβ1-3GlcNAcβ1-3Galβ1-4Glc-PA	Agalacto $V^6HSO_{3\text{-}1,2}Lc_6$	1.7
A6	HSO_3 (6) Galβ1-4GlcNAcβ1-3Galβ1-4Glc-PA; Fucα1 (3)	III^6HSO_3,III^3Fucα-nLc_4	0.4
A7	Neu5Acα2-3Galβ1-3GlcNAcβ1-3Galβ1-4Glc-PA	LST-a	4.6
A8	Galβ1-3GlcNAcβ1-3Galβ1-4Glc-PA (6); Neu5Acα2	LST-b	2.7
A9	Neu5Acα2-6Galβ1-4GlcNAcβ1-3Galβ1-4Glc-PA	LST-c	33.3
A10-1	HSO_3 (6) Galβ1-4GlcNAcβ1-3Galβ1-3GlcNAcβ1-3Galβ1-4Glc-PA	$V^6HSO_{3\text{-}1,2}Lc_6$	0.6
A10-2	Neu5Acα2-3Galβ1-3GlcNAcβ1-3Galβ1-4Glc-PA (6); Neu5Acα2	IV^3NeuAcα,III^6NeuAcα-Lc_4	7.7
A11	Neu5Acα2-3Galβ1-4GlcNAcβ1-3Galβ1-4Glc-PA (3); Fucα1	SLe^x	3.5
A12	Neu5Acα2-3Galβ1-3GlcNAcβ1-3Galβ1-4Glc-PA (4); Fucα1	SLe^a	2.0
A13-1	Neu5Acα2 (6); Neu5Acα2-3Galβ1-3GlcNAcβ1-3Galβ1-4Glc-PA (4); Fucα1	IV^3NeuAcα,III^6NeuAcα,III^4Fucα-Lc_4	0.2
A13-2	HSO_3 (6) Neu5Acα2-6Galβ1-4GlcNAcβ1-3Galβ1-3GlcNAcβ1-3Galβ1-4Glc-PA	VI^6NeuAcα,$V^6HSO_{3\text{-}1,2}Lc_6$	1.6

(Continued)

Table IV. Continued

Fraction	Structure	Abbreviation	Ratio (%)
Acidic			
A14	HSO_3(6) Galβ1-4GlcNAcβ1-3Galβ1-3GlcNAcβ1-3Galβ1-4Glc-PA Fucα1(3)	$V^6HSO_3,V^3Fuc\alpha\text{-}_{1,2}Lc_6$	4.7
A15	HSO_3(6) Galβ1-4GlcNAcβ1-3Galβ1-4GlcNAcβ1-3Galβ1-4Glc-PA Fucα1(3)	$V^6HSO_3,III^3Fuc\alpha\text{-}nLc_6$	0.8
A16-1	Neu5Acα2-3Galβ1-4GlcNAcβ1-3Galβ1-4GlcNAcβ1-3Galβ1-4Glc-PA	$VI^3NeuAc\alpha\text{-}nLc_6$	0.2
A16-2	HSO_3(6) Neu5Acα2-3Galβ1-4GlcNAcβ1-3Galβ1-3GlcNAcβ1-3Galβ1-4Glc-PA Fucα1(3)	$VI^3NeuAc\alpha,V^6HSO_3,V^3Fuc\alpha\text{-}_{1,2}Lc_6$	0.3
A17	HSO_3(6) Galβ1-4GlcNAcβ1-3Galβ1-3GlcNAcβ1-3Galβ1-4Glc-PA Fucα1(3) Neu5Acα2(6)	$V^6HSO_3,V^3Fuc\alpha,III^6NeuAc\alpha\text{-}_{1,2}Lc_6$	0.3
A18	Neu5Acα2-6Galβ1-4GlcNAcβ1-3Galβ1-3GlcNAcβ1-3Galβ1-4Glc-PA	$VI^6NeuAc\alpha,\text{-}_{1,2}Lc_6$	8.9
A19	HSO_3(6) Neu5Acα2-6Galβ1-4GlcNAcβ1-3Galβ1-4GlcNAcβ1-3Galβ1-4Glc-PA Fucα1(3)	$VI^6NeuAc\alpha,V^6HSO_3,III^3Fuc\alpha\text{-}nLc_6$	1.3
A20	HSO_3(6) Galβ1-4GlcNAcβ1-3Galβ1-4GlcNAcβ1-3Galβ1-4Glc-PA Fucα1(3) Fucα1(3)	$V^6HSO_3,V^3Fuc\alpha,III^3Fuc\alpha\text{-}nLc_6$	5.0
A21	HSO_3(6) Neu5Acα2-3Galβ1-4GlcNAcβ1-3Galβ1-4GlcNAcβ1-3Galβ1-4Glc-PA Fucα1(3) Fucα1(3)	$VI^3NeuAc\alpha,V^6HSO_3,V^3Fuc\alpha,III^3Fuc\alpha\text{-}nLc_6$	0.4
A22	Neu5Acα2-6Galβ1-4GlcNAcβ1-3Galβ1-4GlcNAcβ1-3Galβ1-4Glc-PA Fucα1(3)	$VI^6NeuAc\alpha,III^3Fuc\alpha\text{-}nLc_6$	8.5
A23	Neu5Acα2-3Galβ1-4GlcNAcβ1-3Galβ1-4GlcNAcβ1-3Galβ1-4Glc-PA Fucα1(3) Fucα1(3)	$VI^3NeuAc\alpha,V^3Fuc\alpha,III^3Fuc\alpha\text{-}nLc_6$	0.7

(Continued)

Table IV. Continued

Fraction	Structure	Abbreviation	Ratio (%)
Neutral			
N1	Galβ1-4Glc-PA	Lactose	7.7
N2	GlcNAcβ1-3Galβ1-4Glc-PA	Lc_3	4.3
N3	GalNAcβ1-3Galα1-4Galβ1-4Glc-PA	Gb_4	0.4
N4	Galβ1-3GlcNAcβ1-3Galβ1-4Glc-PA	Lc_4	6.8
N5	Galβ1-4GlcNAcβ1-3Galβ1-4Glc-PA	nLc_4	2.3
N6	Fucα1-2Galβ1-3GlcNAcβ1-3Galβ1-4Glc-PA	TypeI H	6.5
N7-1	Galβ1-3GlcNAcβ1-3Galβ1-4Glc-PA 4 Fucα1	Le^a	8.7
N7-2	Galβ1-4GlcNAcβ1-3Galβ1-4Glc-PA 3 Fucα1	Le^x	26.2
N8	GalNAcα1-3Galβ1-3GlcNAcβ1-3Galβ1-4Glc-PA 2 Fucα1	TypeI A	17.6
N9	Fucα1-2Galβ1-4GlcNAcβ1-3Galβ1-4Glc-PA 3 Fucα1	Le^y	0.4
N10-1	Fucα1-2Galβ1-3GlcNAcβ1-3Galβ1-4Glc-PA 4 Fucα1	Le^b	2.8
N10-2	Galβ1-3GlcNAcβ1-3Galβ1-3GlcNAcβ1-3Galβ1-4Glc-PA	Lc_6	0.6
N11	Galβ1-4GlcNAcβ1-3Galβ1-4GlcNAcβ1-3Galβ1-4Glc-PA	nLc_6	0.1
N12-1	GalNAcα1-3Galβ1-3GlcNAcβ1-3Galβ1-4Glc-PA 2 4 Fucα1 Fucα1	A Le^b	1.6
N12-2	Galβ1-3GlcNAcβ1-3Galβ1-3GlcNAcβ1-3Galβ1-4Glc-PA 2 Fucα1	$VI^2Fuc\alpha$-Lc_6	2.4
N13-1	Galβ1-4GlcNAcβ1-3Galβ1-3GlcNAcβ1-3Galβ1-4Glc-PA 3 Fucα1	$V^3Fuc\alpha_{-1,2}Lc_6$	3.1
N13-2	GalNAcα1-3Galβ1-3GlcNAcβ1-3Galβ1-3GlcNAcβ1-3Galβ1-4Glc-PA 2 Fucα1	$VI^3GalNAc\alpha$,$VI^2Fuc\alpha$-Lc_6	4.4
N14	Galβ1-4GlcNAcβ1-3Galβ1-4GlcNAcβ1-3Galβ1-4Glc-PA 3 Fucα1	$III^3Fuc\alpha$-nLc_6	0.5
N15	Galβ1-4GlcNAcβ1-3Galβ1-4GlcNAcβ1-3Galβ1-4Glc-PA 3 3 Fucα1 Fucα1	$V^3Fuc\alpha$,$III^3Fuc\alpha$-nLc_6	3.6

Table V. Estimated structures of acidic PA-oligosaccharides from colon cancer cells of case 2

Fraction	Structure	Abbreviation	Ratio (%)
A1	HSO_3-3Galβ1-4Glc-PA	SM3	1.4
A2	Neu5Acα2-3Galβ1-4Glc-PA	GM3	54.2
A3	Neu5Acα2-8Neu5Acα2-3Galβ1-4Glc-PA	GD3	5.4
A4	GalNAcβ1-4Galβ1-4Glc-PA 3 Neu5Acα2-8Neu5Acα2	GD2	0.2
A5	Neu5Acα2-3Galβ1-4GlcNAcβ1-3Galβ1-4Glc-PA	SPG	2.6
A6	Galβ1-3GalNAcβ1-4Galβ1-4Glc-PA 3 3 Neu5Acα2 Neu5Acα2	GD1a	1.7
A7	Neu5Acα2-6Galβ1-4GlcNAcβ1-3Galβ1-4Glc-PA	LST-c	26.9
A8-1	Neu5Acα2-3Galβ1-4GlcNAcβ1-3Galβ1-4Glc-PA 3 Fucα1	SLe^x	0.6
A8-2	Neu5Acα2-6Galβ1-4GlcNAcβ1-3Galβ1-4Glc-PA 2 Fucα1	$IV^2Fuc\alpha,IV^6NeuAc\alpha$-$nLc_4$	0.1
A9-1	Neu5Acα2-3Galβ1-3GlcNAcβ1-3Galβ1-4Glc-PA 4 Fucα1	SLe^a	2.3
A9-2	Galβ1-3GalNAcβ1-4Galβ1-4Glc-PA 3 3 Neu5Acα2 Neu5Acα2-8Neu5Acα2	GT1b	0.7
A10	Neu5Acα2-3Galβ1-4GlcNAcβ1-3Galβ1-4GlcNAcβ1-3Galβ1-4Glc-PA	$VI^3NeuAc\alpha$-nLc_6	1.6
A11-1	HSO_3-3Galβ1-4GlcNAcβ1-3Galβ1-4GlcNAcβ1-3Galβ1-4Glc-PA 3 3 Fucα1 Fucα1	$VI^3HSO_3,V^3Fuc\alpha,III^3Fuc\alpha$-$nLc_6$	0.2
A11-2	Neu5Acα2-6Galβ1-4GlcNAcβ1-3Galβ1-4GlcNAcβ1-3Galβ1-4Glc-PA	$VI^6NeuAc\alpha$-nLc_6	0.4
A12	HSO_3 6 Galβ1-4GlcNAcβ1-3Galβ1-4GlcNAcβ1-3Galβ1-4Glc-PA 3 3 Fucα1 Fucα1	$V^6HSO_3,V^3Fuc\alpha,III^3Fuc\alpha$-$nLc_6$	0.3
A13	Neu5Acα2-6Galβ1-4GlcNAcβ1-3Galβ1-4GlcNAcβ1-3Galβ1-4Glc-PA 3 Fucα1	$VI^6NeuAc\alpha,III^3Fuc\alpha$-$nLc_6$	1.3

on the map to the positions of standard PA-oligosaccharides, all the peaks, except A11-1 and A12 in CCs, were matched to the reference standard oligosaccharides we had already acquired. Their structures were also confirmed by mass spectrometry analyses. The structures of the acidic GSLs of CCs from case 2 are listed in Table V. Expression of SM3 (A1), GM3 (A2), and GD3 (A3) in CCs and NCs are very similar. Other ganglio series GSLs such as GD1a (A6), GM1 (A14), and GD1b (A15) were decreased or disappeared in malignant transformation. LST-c (A7) was increased, and other neolacto and lacto series GSLs, SLe^x (A8-1), $IV^2Fuc\alpha IV^6NeuAc\alpha$-$nLc_4$ (A8-2), SLe^a (A9-1), $VI^3NeuAc\alpha$-nLc_6 (A10), A11-1, $VI^6NeuAc\alpha$-nLc_6 (A11-2), A12, and $VI^6NeuAc\alpha III^3Fuc\alpha$-$nLc_6$ (A13) appeared in carcinogenesis, as minor components. Unmatched oligosaccharides, A11-1 and A12 in CCs, were monosulfated, as evidenced by mass spectrometry analyses, and A12 of case

2 was identical to A20 of case 1 as judged by 2D mapping and mass spectrometry analysis.

The structure of A11-1 was monosulfated, difucosylated, on a hexasaccharide backbone, as evidence by mass spectrometry analysis. The elution position of A11-1 on two types of HPLC (NP 5.87, RP 3.37) corresponded to the newly synthesized monosulfated difucosylated PA-oligosaccharides, HSO_3-3Galβ1-4(Fucα1-3)GlcNAcβ1-3Galβ1-4(Fucα1-3)GlcNAcβ1-3Galβ1-4Glu, (3′-sulfo-V^3FucαIII^3Fucα-nLc_6), and HSO_3-3Galβ1-3(Fucα1-4)GlcNAcβ1-3Galβ1-4(Fucα1-3)GlcNAcβ1-3Galβ1-4Glu (3′-sulfo-V^4FucαIII^3Fucα-$_{2,1}Lc_6$), but not other isomers (Table II). Further analysis to determine the structure of A11-1 could not be performed due to the limited amount of A11-1. However, the former structure ending in a 3′-sulfo Le^x structure is more probable as described below. Among the GSLs of CCs from case 2 having a hexasaccharide backbone, derivatives of nLc_6 are dominant, and those being of a type-1 and –type-2 hybrid are very minor (data not shown). A further reason concerns the substrate specificity of sulfotransferase. Four kinds of βGal-3-*O*-sulfotransferases (Gal3STs), Gal3ST-1, Gal3ST-2, Gal3ST-3, and Gal3ST-4, catalyzing the transfer of a sulfate group from the donor substrate PAPS to the C3 position of the nonreducing terminal Gal residue of carbohydrate chains, have been identified (Honke et al. 1997, 2001; El-Fasakhany et al. 2001; Seko et al. 2001; Suzuki et al. 2001). Among them, Gal3ST-2 and Gal3ST-3 are capable of transferring a sulfate residue to the terminal galactose of type-1 or type-2 lactosamine chains. However, type 2 chains serve as good acceptors, whereas type 1 chains serve as poor acceptors for Gal3ST3. In terms of Gal3ST2, Honke et al. (2001) demonstrated using PA-nLc_4 and PA-Lc_4 as model substrates that it acts on both type 1 chains and type 2 chains. Although we also confirmed this substrate specificity of Gal3ST2 using the same type-1 and type-2 tetrasaccharides, we found that when we synthesized the 3′-sulfated standard oligosaccharides using nLc_6, Lc_6, and two types of type-1 and type-2 hybrid ($_{1,2}Lc_6$ and $_{2,1}Lc_6$) as acceptors (data not shown), Gal3ST2 much prefers to add sulfate to the terminal galactose ending type 2 chains of hexasaccharides above the terminal galactose ending type 1 chains of hexasaccharides. The predicted structures of the acidic GSLs of CCs from case 2 are presented in Table V.

Discussion

In our recent study, we identified 27 and 28 kinds of acidic and neutral GSLs, respectively, from CCs and NCs of 16 patients and obtained quantitatively and qualitatively precise structures (Misonou et al. 2009). Even though extensive structural analyses of CCs and NCs were performed, we found in subsequent structural analyses that CCs from two patients had a number of GSLs, which could not be found in the CCs and NCs from the other patients, while the NCs from the same patients displayed normal GSL structures. The CCs from these two patients are estimated to have low metastatic potential. We demonstrated that the carbohydrate structures of these CCs have a common feature in that both include sulfated oligosaccharides linked at two different positions: the C6 position of GlcNAc and the C3 position of galactose, besides SM3. Furthermore, the structures from the CCs of case 1, but not case 2, include derivatives of $_{1,2}Lc_6$.

SM3 was the only sulfated GSL found in both the CCs and NCs of many of the cases. However, in the CCs from two cases, sulfate is linked to the C6 position of subterminal GlcNAc and to the C3 position of terminal galactose with or without sialylation or fucosylation, to form a variety of sulfated structures. GSLs from case 1 include a variety of GSLs sulfated at 6-*O*-GlcNAc forming 6-sulfo lactosamine (A10-1, A15), 6-sulfo Le^x (A6, A14, A17, A20), 6′-sialyl 6-sulfo lactosamine (A13-2, A19), 3′-sialyl 6-sulfo Le^x (A16-2, A21), and one GSL (SM3 apart) sulfated at C3 galactose to form 3′-sulfo lactosamine (A3). Furthermore, two unusual structures, sulfated at terminal GlcNAc (A5) and sulfated at the subterminal fifth GlcNAc with sialylation at an internal third GlcNAc (A17) on a hexasaccharide backbone, were also detected. Generation of sulfated terminal GlcNAc (A5) is thought to be due to failure of the addition of galactose to sulfated GlcNAc residues rather than an artifact of removal of galactose by galactosidase because GSLs terminated at the fifth GlcNAc have not been found in CCs or NCs in our study with the exception of A5. In the CCs from case 2, a single oligosaccharide sulfated at the C6 position of GlcNAc and a single oligosaccharide sulfated at the C3 position of galactose were found, forming 6-sulfo Le^x (A12) and 3′-sulfo Le^x (A11-1), respectively. To our knowledge, this is the first report of the presence of the various sulfated GSLs including 6-*O*-sulfation of GlcNAc and 3′-sulfation of terminal galactose (except for SM3), although some of the structures are found in keratan sulfate as well as *N*-linked and *O*-linked glycans (Dickenson et al. 1992; Yuen et al. 1992; Hemmerich et al. 1995; Murakami et al. 2007).

In terms of GSLs having hexasaccharide backbones, oligosaccharides extending type 2 chains or type 1 chains to nLc_4, such as V^3FucαIII^3Fucα-nLc_6, VI^3NeuAcα-nLc_6, VI^6NeuAcαIII^3Fucα-nLc_6, and V^4FucαIII^3Fucα-$_{2,1}Lc_6$, are mostly observed in both CCs and NCs. However, elongation of type 1 or type 2 chains to Lc_4 to form Lc_6 or $_{1,2}Lc_6$ was found in the CCs from case 1. Besides case 1, fucosylated or sialylated derivatives of these structures were also found in CCs from two other patients as described in our previous report (cases 7 and 16) (Misonou et al. 2009). Furthermore, the presence of the derivative of Lc_6, V^4FucαIII^4Fucα-Lc_6, in various human cancer tissues has been reported (Stroud et al. 1991). Although GSLs having the structure of $_{1,2}Lc_6$ have been isolated from human meconium (Karlsson and Larson 1981) (but not from any other human tissues to date), the presence of these structures in cancer tissues or cells suggests that the structures can be generated in particular types of cells.

In our previous and subsequent analyses, seven patients were classified as stage II according to the TNM classification because the tumor invaded through the muscularis propria without any lymph node metastases and distant organ metastases. Our study showed that the CCs had the sulfated GSLs in two of these cases. The physiological relevance of the sulfated GSLs in CCs is not clear at present. However, given the clinical features of the cases and expression pattern which show that a variety and high levels of sulfated GSLs are expressed in CCs of undoubtedly low metastatic potential (case 1), we propose a hypothesis that they may, at least in part, be involved in the observed low metastatic potential (even though the number of samples is still small). The interaction between sulfated GSLs on the surface of cancer cells and lectins, such as selectins, is worthy of discussion given that sulfated oligosaccharide determinants have been shown to function as ligands of selectins. In particular, the sialyl 6-sulfo

Lewis X determinant is highly expressed on high endothelial venules of human peripheral lymph nodes, serves as a major L-selectin ligand, and is intimately involved in lymphocyte homing (Hemmerich et al. 1995; Mitsuoka et al. 1997, 1998). Furthermore, 3′-sulfo Le^x/Le^a determinants were also shown to be more potent ligands for L- and E-selectin than 3′-sialyl Le^x/Le^a (Green et al. 1992; Yuen et al. 1992, 1994; Feizi and Galustian 1999). GSLs having the former and latter oligosaccharide determinants were found in the CCs of case 1 (A16-2, A21) and case 2 (A11-1). Hence, it is possible that the tight interaction between the above sulfated oligosaccharides on the surface of CCs and L-selectin on the surface of the lymphocytes infiltrating the cancer tissues inhibit migration of the cancer cells into blood or lymph circulation. Furthermore, attention is also warranted to the commonly expressed sulfated GSLs of both sets of CCs, namely 6-sulfo Le^x. The presence of ligands of the 6-sulfo Le^x determinant has not been confirmed to date but if ligands exist in cancerous tissues, in particular, in the extracellular matrix, they may play an important role in cancer metastasis.

Validation of the proposal by increasing the number of samples for which structural analysis is complete is essential. However, this may be a relatively time-consuming undertaking given the rarity of CCs similar to those of case 1 judged to have low metastatic potential. Functional analysis of sulfated GSLs is also important in order to examine the proposal.

Material and methods

All human specimens were obtained from Osaka Medical Center for Cancer and Cardiovascular Diseases. This study was approved by the Local Ethics Committee of Osaka Medical Center for Cancer and Cardiovascular Diseases. Informed consent was obtained from the patients. The majority of the experimental procedures including purification of CCs and NCs, isolation of GSLs, preparation and separation of PA-oligosaccharides, and mass spectrometry analyses have been reported previously (Misonou et al. 2009). In brief, CCs and NCs were highly purified from primary lesions of colon cancers and their surrounding normal colon mucosa, respectively, using the epithelial cell marker, CD326, and magnetic beads. The tissues were dissected into small blocks and incubated in the DMEM/F12 medium containing 2 mg/mL collagenase (Sigma, St. Louis, MO). The digested cells were resuspended in PBS containing 2 mM EDTA and 0.5% BSA, and CD326-positive cells were positively selected using magnetically labeled microbeads (Miltenyi Biotec, Bergisch Gladbach, Germany) according to the manufacturer's protocol.

The neutral and acidic GSLs were extracted from the cells and digested with recombinant endoglycoceramidase II from *Rhodococcus* Sp. (Takara Bio Inc. Shiga, Japan) (Ito and Yamagata 1989). Released oligosaccharides were labeled with 2-aminopyridine (2-AP) (Natsuka and Hase 1998).

PA-oligosaccharides were separated on a Shimazu LC-20A HPLC system equipped with a Waters 2475 fluorescence detector. Normal-phase HPLC was performed on a TSK gel Amide-80 column (0.2 × 25 cm, Tosoh, Tokyo, Japan). The molecular size of each PA-oligosaccharide is given in glucose units (Gu) based on the elution times of PA-isomaltooligosaccharides. Reversed-phase HPLC was performed on a TSK gel ODS-80Ts column (0.2 × 15 cm, Tosoh). The retention time of each PA-oligosaccharide is given in glucose units based on the elution times of PA-isomaltooligosaccharides. Thus, a given compound on these two columns provides a unique set of Gu (amide) and Gu (ODS) values, which correspond to coordinates of the 2D map. PA-oligosaccharides were analyzed by LC/ESI MS/MS. High-performance liquid chromatography was performed on a Paradigm MS4 equipped with a Magic C18 column (0.2 × 50 mm, Michrome BioResource, Auburn, CA).

Standard PA-oligosaccharides

The structures, abbreviations, and glucose units of authentic PA-oligosaccharides, used in this study are listed in Table II, which include PA-oligosaccharides commercially purchased, kindly donated, prepared from our previous study or synthesized in this study. Two kinds of type-1 and type-2 hybrid hexasaccharides, Galβ1-3GlcNAcβ1-3Galβ1-4GlcNAcβ1-3Galβ1-4Glc and Galβ1-4GlcNAcβ1-3Galβ1-3GlcNAcβ1-3Galβ1-4Glc are abbreviated as $_{2,1}Lc_6$ and $_{1,2}Lc_6$, respectively, in order of linkage type of the fourth and sixth galactose.

Four kinds of 3′-monosulfated, difucosylated oligosaccharides-PA having hexasaccharide backbones were synthesized in this study. $III^3Fuc\alpha$-nLc_6-PA was already acquired from the previous study. Galβ1-3GlcNAcβ1-3Galβ1-4GlcNAcβ1-3Galβ1-4Glc-PA ($_{2,1}Lc_6$) was prepared from Galβ1-3GlcNAcβ1-3Galβ1-4(Fucα1-3)GlcNAcβ1-3Galβ1-4Glc-PA ($III^3Fuc\alpha$-$_{2,1}Lc_6$) by releasing the fucosyl residue with bovine kidney fucosidase. Lc_6-PA and Galβ1-4(Fucα1-3)GlcNAcβ1-3Galβ1-3GlcNAcβ1-3Galβ1-4Glc-PA ($V^3Fuc\alpha$-$_{1,2}Lc_6$) were obtained in the process of analyzing the CCs reported in this study. Galβ1-4GlcNAcβ1-3Galβ1-3GlcNAcβ1-3Galβ1-4Glc-PA ($_{1,2}Lc_6$) was obtained from Galβ1-4(Fucα1-3)GlcNAcβ1-3Galβ1-3GlcNAcβ1-3Galβ1-4Glc-PA ($V^3Fuc\alpha$-$_{1,2}Lc_6$) by releasing the fucosyl residue with α1,3/4-fucosidase. Human β-Gal-3-*O*-sulfotransferase 2 (Gal3ST-2, GP3ST) expression plasmid, pcXN2-GP3ST, and human fucosyltransferase III (Fut III) expression plasmid, pcDNA Fut-III, were used to obtain 3′-sulfated and α1,3/4-fucosylated standard oligosaccharides (Ikeda et al. 2001). COS 7 cells (1×10^7) were transfected with 8 μg each of expression vector and 20 μL of Lipofectamine 2000 (Invitrogen, Carlsbad, CA). After 24 h, the cells were washed, harvested with phosphate-buffered saline, and sonicated in 50 μL of ice-cold 20 mM HEPES buffer (pH 7.4), 1% Triton X-100 for 5 min. After centrifugation at 12,000 × *g* for 10 min, the supernatants were used as sources of GP3ST and Fut-III. 3′-sulfo,$III^3Fuc\alpha$-nLc_6-PA, 3′-sulfo-Lc_6-PA, 3′-sulfo-$_{1,2}Lc_6$-PA, and 3′-sulfo-$_{2,1}Lc_6$-PA were synthesized by sulfation of $III^3Fuc\alpha$-nLc_6-PA, Lc_6-PA, $_{1,2}Lc_6$-PA, and $_{2,1}Lc_6$-PA, respectively, using COS 7 cell lysate transfected with pcXN2-GP3ST. The incubation mixture of GP3ST contained the following components in a total volume of 10 μL: 100 mM MES buffer (pH 6.2) 10 mM $MnCl_2$, 1% Lubrol PX, 1 mM PAPS, 1 μL of enzyme source, and an appropriate volume of each acceptor substrate. After incubation of 2–16 h, the reactions were terminated by boiling for 3 min and reaction mixtures were subjected to reversed-phase HPLC. The fraction containing 3′-sulfated PA-oligosaccharides was further subjected to mass spectrometry analysis and normal phase HPLC to obtain glucose units. The four kinds of 3′-sulfated PA-oligosaccharides were further fucosylated to obtain 3′-sulfo-$V^3Fuc\alpha III^3Fuc\alpha$-$nLc_6$-PA,

3′-sulfo-V^{4}FucαIII^{4}Fucα-Lc$_6$-PA, 3′-sulfo-V^{3}FucαIII^{4}Fucα-$_{1,2}$Lc$_6$-PA, and 3′-sulfo-V^{4}FucαIII^{3}Fucα-$_{2,1}$Lc$_6$-PA using COS7 cell lysate transfected with pcDNA Fut-III. The incubation mixture of Fut-III contained the following components in a total volume of 10 μL: 50 mM cacodylate buffer, pH 6.5, 5 mM ATP, 25 mM $MnCl_2$, 10 mM L-fucose, 0.075 mM GDP-fucose, 1 μL of enzyme source, and an appropriate volume of each acceptor substrate. The reaction mixtures were subjected to two different kinds of HPLC and fractions corresponding to 3′-sulfated difucosylated oligosaccharides, as judged by mass spectrometry analysis, were collected.

Glycosidase digestion

Sialyl PA-oligosaccharides were digested with 2 U/mL of α2,3-sialidase from *Salmonella typhimurium* (Takara Bio Inc.) or 2 U/mL of α-sialidase from *Arthrobacter ureafaciens* (Nacalai, Kyoto, Japan) in the 100 mM sodium acetate buffer, pH 5.5, for 2 h at 37°C (condition 1). Under these conditions, α2,3-sialidase specifically digests sialic acid α2–3 linked to the terminal residue, but not sialic acid with an α2-6 linkage whilst *Arthrobacter* α-sialidase digests both linkages independent of the linkage position. However, under conditions using 10 U/mL for 16 h (condition 2), even so-called α2,3-sialidase can hydrolyze sialic acid α2–6 linked to the terminal residue, but not sialic acid linked to a nonterminal residue. Hence, we were able to conclude the linkage position of sialic acid using these two enzymes as follows: (1) when sialyl PA-oligosaccharide was cleaved by α2,3-sialidase in condition 1, sialic acid was concluded to be linked to the terminal residue through an α2-3 linkage. (2) When sialyl PA-oligosaccharide was cleaved by α2,3-sialidase in condition 2, but not in condition 1, sialic acid was concluded to be linked to the terminal residue through an α2-6 linkage. (3) When sialyl PA-oligosaccharide was cleaved by *Arthrobacter* α-sialidase in condition 1 but not by α2,3-sialidase even in condition 2, sialic acid was concluded to be linked to a nonterminal residue.

In other glycosidase digests, PA-oligosaccharides were digested with (a) 0.2 mU/mL of α1,3/4-fucosidase from *Streptomyces* sp. 142 (Takara Bio Inc.) in the 100 mM sodium acetate buffer, pH 5.5, for 2 h at 37°C; (b) 0.4 U/mL β1,4-galactosidase from *Streptococcus pneumonia* (Prozyme, San Leandro, CA) in the 100 mM sodium citrate buffer, pH 6.0, for 2 h at 37°C; (c) 10 U/mL of β-*N*-acetylhexosaminidase from Jack bean (Seikagaku Kogyo, Tokyo, Japan) in the 100 mM sodium citrate buffer, pH 5.0, for 16 h at 37°C; (d) 4 U/mL of α1,2-fucosidase from *Corynebacterium* sp. (Takara Bio Inc.) in the 100 mM sodium phosphate buffer, pH 8.5, for 16 h at 37°C; (e) 0.5 U/mL of endo-β-galactosidase from *Escherichia freundii* (Seikagaku Kogyo) in the 100 mM sodium acetate buffer, pH 5.8, for 16 h at 37°C; (f) 10 U/mL of α-fucosidase from bovine kidney (Sigma, St. Louis, MI) in the 100 mM sodium acetate buffer, pH 5.5, for 16 h at 37°C; (g) 0.2 mU/mL of lacto-*N*-biosidase from *streptomyces* sp 142 (Takara Bio Inc.) in the 100 mM sodium acetate buffer, pH 5.5, for 2 h at 37°C; (h) 2 U/mL of α-*N*-acetylgalactosaminidase from *Acremonium* sp. (Seikagaku Kogyo) in the 100 mM sodium citrate buffer, pH 4.5, for 2 h at 37°C; (i) 10 U/mL of β-galactosidase from Jack bean (Seikagaku Kogyo) in the 100 mM sodium citrate buffer, pH 3.5, for 16 h at 37°C; (J) 1 U/mL of β-*N*-acetylhexosaminidase from human placenta (Sigma) in the 100 mM sodium citrate buffer, pH 4.3, for 16 h at 37°C. All the reactions were terminated by boiling the solutions for 3 min at 100°C.

Methanolysis of sulfated PA-glycans

PA-Glycans were methanolyzed with 10 μL of 50 mM HCl in methanol at 37°C for 3 h (Murakami et al. 2007). After the reaction, the products were concentrated to dryness three times with 100 μL of methanol.

Funding

The Ministry of Health, Labour and Welfare of Japan.

Acknowledgement

We thank Shunji Natsuka for useful discussions and critical comments on the manuscript.

Conflict of interest statement

None declared.

Abbreviations

CCs, colorectal cancer cells; HPLC, high-performance liquid chromatography; NCs, normal colorectal epithelial cells.

Reference

Bullock SL, Fletcher JM, Beddington RS, Wilson VA. 1998. Renal agenesis in mice homozygous for a gene trap mutation in the gene encoding heparan sulfate 2-sulfotransferase. *Genes Dev.* 12(12):1894–1906.

Dickenson JM, Huckerby TN, Nieduszynski IA. 1992. Skeletal keratan sulphate chains isolated from bovine intervertebral disc may terminate in alpha(2-6)-linked *N*-acetylneuraminic acid. *Biochem J.* 282(Pt 1):267–271.

El-Fasakhany FM, Uchimura K, Kannagi R, Muramatsu T. 2001. A novel human Gal-3-*O*-sulfotransferase: Molecular cloning, characterization, and its implications in biosynthesis of (SO(4)-3)Galbeta1–4(Fucalpha1–3)GlcNAc. *J Biol Chem.* 276(29):26988–26994.

Feizi T, Galustian C. 1999. Novel oligosaccharide ligands and ligand-processing pathways for the selectins. *Trends Biochem Sci.* 24(10):369–372.

Forsberg E, Pejler G, Ringvall M, Lunderius C, Tomasini-Johansson B, Kusche-Gullberg M, Eriksson I, Ledin J, Hellman L, Kjellen L. 1999. Abnormal mast cells in mice deficient in a heparin-synthesizing enzyme. *Nature.* 400(6746):773–776.

Fukushi Y, Nudelman E, Levery SB, Hakomori S, Rauvala H. 1984. Novel fucolipids accumulating in human adenocarcinoma: III. A hybridoma antibody (FH6) defining a human cancer-associated difucoganglioside (VI3NeuAcV3III3Fuc2nLc6). *J Biol Chem.* 259(16):10511–10517.

Green PJ, Tamatani T, Watanabe T, Miyasaka M, Hasegawa A, Kiso M, Yuen CT, Stoll MS, Feizi T. 1992. High affinity binding of the leucocyte adhesion molecule L-selectin to 3′-sulphated-Le(a) and -Le(x) oligosaccharides and the predominance of sulphate in this interaction demonstrated by binding studies with a series of lipid-linked oligosaccharides. *Biochem Biophys Res Commun.* 188(1):244–251.

Hakomori S. 1989. Aberrant glycosylation in tumors and tumor-associated carbohydrate antigens. *Adv Cancer Res.* 52:257–331.

Hakomori S. 1996. Tumor malignancy defined by aberrant glycosylation and sphingo(glyco)lipid metabolism. *Cancer Res.* 56(23):5309–5318.

Hakomori S. 2002. Glycosylation defining cancer malignancy: New wine in an old bottle. *Proc Natl Acad Sci USA.* 99(16):10231–10233.

Hemmerich S, Bistrup A, Singer MS, van Zante A, Lee JK, Tsay D, Peters M, Carminati JL, Brennan TJ, Carver-Moore K, et al. 2001. Sulfation of

L-selectin ligands by an HEV-restricted sulfotransferase regulates lymphocyte homing to lymph nodes. *Immunity.* 15(2):237–247.

Hemmerich S, Leffler H, Rosen SD. 1995. Structure of the *O*-glycans in GlyCAM-1, an endothelial-derived ligand for l-selectin. *J Biol Chem.* 270(20):12035–12047.

Honke K, Hirahara Y, Dupree J, Suzuki K, Popko B, Fukushima K, Fukushima J, Nagasawa T, Yoshida N, Wada Y, et al. 2002. Paranodal junction formation and spermatogenesis require sulfoglycolipids. *Proc Natl Acad Sci USA.* 99(7):4227–4232.

Honke K, Tsuda M, Hirahara Y, Ishii A, Makita A, Wada Y. 1997. Molecular cloning and expression of cDNA encoding human 3′-phosphoadenylylsulfate:galactosylceramide 3′-sulfotransferase. *J Biol Chem.* 272(8):4864–4868.

Honke K, Tsuda M, Koyota S, Wada Y, Iida-Tanaka N, Ishizuka I, Nakayama J, Taniguchi N. 2001. Molecular cloning and characterization of a human beta-Gal-3′-sulfotransferase that acts on both type 1 and type 2 (Gal beta 1-3/1-4GlcNAc-R) oligosaccharides. *J Biol Chem.* 276(1):267–274.

Humphries DE, Wong GW, Friend DS, Gurish MF, Qiu WT, Huang C, Sharpe AH, Stevens RL. 1999. Heparin is essential for the storage of specific granule proteases in mast cells. *Nature.* 400(6746):769–772.

Ikeda N, Eguchi H, Nishihara S, Narimatsu H, Kannagi R, Irimura T, Ohta M, Matsuda H, Taniguchi N, Honke K. 2001. A remodeling system of the 3′-sulfo-Lewis a and 3′-sulfo-Lewis x epitopes. *J Biol Chem.* 276(42):38588–38594.

Ishizuka I. 1997. Chemistry and functional distribution of sulfoglycolipids. *Prog Lipid Res.* 36(4):245–319.

Ito M, Yamagata T. 1989. Purification and characterization of glycosphingolipid-specific endoglycosidases (endoglycoceramidases) from a mutant strain of Rhodococcus sp. Evidence for three molecular species of endoglycoceramidase with different specificities. *J Biol Chem.* 264(16):9510–9519.

Karlsson KA, Larson G. 1981. Molecular characterization of cell surface antigens of fetal tissue. Detailed analysis of glycosphingolipids of meconium of a human O Le(a–b+) secretor. *J Biol Chem.* 256(7):3512–3524.

Korekane H, Tsuji S, Noura S, Ohue M, Sasaki Y, Imaoka S, Miyamoto Y. 2007. Novel fucogangliosides found in human colon adenocarcinoma tissues by means of glycomic analysis. *Anal Biochem.* 364(1):37–50.

Misonou Y, Shida K, Korekane H, Seki Y, Noura S, Ohue M, Miyamoto Y. 2009. Comprehensive Clinico-Glycomic Study of 16 Colorectal Cancer Specimens: Elucidation of aberrant glycosylation and ts mechanistic causes in colorectal cancer cells. *J Proteome Res.* 8(6):2990–3005.

Mitsuoka C, Kawakami-Kimura N, Kasugai-Sawada M, Hiraiwa N, Toda K, Ishida H, Kiso M, Hasegawa A, Kannagi R. 1997. Sulfated sialyl Lewis X, the putative l-selectin ligand, detected on endothelial cells of high endothelial venules by a distinct set of anti-sialyl Lewis X antibodies. *Biochem Biophys Res Commun.* 230(3):546–551.

Mitsuoka C, Sawada-Kasugai M, Ando-Furui K, Izawa M, Nakanishi H, Nakamura S, Ishida H, Kiso M, Kannagi R. 1998. Identification of a major carbohydrate capping group of the L-selectin ligand on high endothelial venules in human lymph nodes as 6-sulfo sialyl Lewis X. *J Biol Chem.* 273(18):11225–11233.

Murakami T, Natsuka S, Nakakita S, Hase S. 2007. Structure determination of a sulfated *N*-glycans, candidate for a precursor of the selectin ligand in bovine lung. *Glycoconj J.* 24(4–5):195–206.

Natsuka S, Hase S. 1998. Analysis of *N*- and *O*-glycans by pyridylamination. *Methods Mol Biol.* 76:101–113.

Ono M, Hakomori S. 2004. Glycosylation defining cancer cell motility and invasiveness. *Glycoconj J.* 20(1):71–78.

Seko A, Hara-Kuge S, Yamashita K. 2001. Molecular cloning and characterization of a novel human galactose 3-*O*-sulfotransferase that transfers sulfate to gal beta 1→3galNAc residue in *O*-glycans. *J Biol Chem.* 276(28):25697–25704.

Stroud MR, Levery SB, Nudelman ED, Salyan ME, Towell JA, Roberts CE, Watanabe M, Hakomori S. 1991. Extended type 1 chain glycosphingolipids: Dimeric Lea (III4V4Fuc2Lc6) as human tumor-associated antigen. *J Biol Chem.* 266(13):8439–8446.

Suzuki A, Hiraoka N, Suzuki M, Angata K, Misra AK, McAuliffe J, Hindsgaul O, Fukuda M. 2001. Molecular cloning and expression of a novel human beta-Gal-3-*O*-sulfotransferase that acts preferentially on *N*-acetyllactosamine in *N*- and *O*-glycans. *J Biol Chem.* 276(26):24388–24395.

Tangemann K, Bistrup A, Hemmerich S, Rosen SD. 1999. Sulfation of a high endothelial venule-expressed ligand for L-selectin. Effects on tethering and rolling of lymphocytes. *J Exp Med.* 190(7):935–942.

Yuen CT, Bezouska K, O'Brien J, Stoll M, Lemoine R, Lubineau A, Kiso M, Hasegawa A, Bockovich NJ, Nicolaou KC, et al. 1994. Sulfated blood group Lewis(a). A superior oligosaccharide ligand for human e-selectin. *J Biol Chem.* 269(3):1595–1598.

Yuen CT, Lawson AM, Chai W, Larkin M, Stoll MS, Stuart AC, Sullivan FX, Ahern TJ, Feizi T. 1992. Novel sulfated ligands for the cell adhesion molecule e-selectin revealed by the neoglycolipid technology among *O*-linked oligosaccharides on an ovarian cystadenoma glycoprotein. *Biochemistry* 31(38):9126–9131.

research articles Journal of proteome research

Comprehensive Clinico-Glycomic Study of 16 Colorectal Cancer Specimens: Elucidation of Aberrant Glycosylation and Its Mechanistic Causes in Colorectal Cancer Cells

Yoshiko Misonou,[†] Kyoko Shida,[†] Hiroaki Korekane,[‡] Yosuke Seki,[§] Shingo Noura,[§] Masayuki Ohue,[§] and Yasuhide Miyamoto*,[†]

Department of Immunology, Osaka Medical Center for Cancer and Cardiovascular Diseases, 1-3-2 Nakamichi, Higashinari-ku, Osaka 537-8511, Japan, Department of Disease Glycomics, Research Institute for Microbial Diseases, Osaka University, 3-1, Yamadaoka, Suita 565-0871, Japan, and Department of Surgery, Osaka Medical Center for Cancer and Cardiovascular Diseases, 1-3-3 Nakamichi, Higashinari-ku, Osaka 537-8511, Japan

Received February 5, 2009

The structures of neutral and acidic glycosphingolipids from both normal colorectal epithelial cells and colorectal cancer cells, which were highly purified with the epithelial cell marker CD326, have been analyzed. The analysis was performed on samples from 16 patients. The carbohydrate moieties from glycosphingolipids were released by endoglycoceramidase II, labeled by pyridylamination, and identified using two-dimensional mapping and mass spectrometry. The structures from normal colorectal epithelial cells are characterized by dominant expression of neutral type-1 chain oligosaccharides. Three specific alterations were observed in malignant transformation; increased ratios of type-2 oligosaccharides, increased α2−3 and/or α2−6 sialylation and increased α1−2 fucosylation. Although the degree of alteration varies case to case, we found that two characteristic alterations tend to be associated with clinical features. One is a shift from type-1 dominant normal colorectal epithelial cells to type-2 dominant colorectal cancer cells. This shift was found in 5 patients having hepatic metastasis. The other is specific elevation of α2−3 sialylation observed in 2 cases exhibiting high serum levels of CA19−9. Examination of the activities of the related glycosyltransferases revealed that while some alterations could be accounted for by changes in the activities of related glycosyltransferases others could not. Although the number of cases analyzed is small, these findings provide valuable information which will help in the elucidation of the mechanism of synthesis of aberrant glycosylation and its involvement in cancer malignancy.

Keywords: colorectal cancer • glycosphingolipid • metastasis • mass spectrometry • two-dimensional mapping • CA19−9 • clinical samples

Introduction

Extensive studies on the oligosaccharide structures of glycosphingolipids (GSLs) in cancers have revealed that aberrant glycosylation occurs in essentially all types of human cancers.[1] Subsequent biochemical and physiological studies indicated that some of the altered oligosaccharide moieties are involved in cancer malignancy such as metastasis and invasion.[2−4] Although elucidation of altered oligosaccharides in carcinogenesis has been crucial, the analyses have not always been performed in a highly accurate and comprehensive manner because of the number of limitations at the time of analysis in terms of both the materials themselves and the conventional analytical techniques, as mentioned below. Therefore, to further pursue the association between aberrant glycosylation and cancer malignancy, reinvestigation of altered glycosylation in carcinogenesis is warranted assuming the problems can be overcome.

In the previous studies, bulk cancerous tissues and normal tissues were used as sources for structural analyses of GSLs.[5−11] However, because both cancer and normal tissues are composed of multiple subpopulations of cells, such as stromal cells, inflammatory cells and angiogenic elements, the analyzed structures from bulk tissues do not reflect those of cancer cells and/or normal epithelial cells. Hence, recently, laser microdissection (LMD) techniques have been widely used for trnascriptome and proteome analyses of cancerous cells. We have previously reported the effectiveness of LMD in cancer glycomic studies.[12] However, subsequent careful evaluation of LMD as a model in cancer glycomic studies of normal and cancerous

* To whom correspondence should be addressed. Yasuhide Miyamoto, Department of Immunology, Osaka Medical Center for Cancer and Cardiovascular Diseases, 1-3-2 Nakamichi, Higashinari-ku, Osaka 537-8511, Japan. Tel: +81-6-6972-1181. Fax:+81-6-6972-7749. E-mail: miyamoto-ya@mc.pref.osaka.jp.

† Department of Immunology, Osaka Medical Center for Cancer and Cardiovascular Diseases.

‡ Osaka University.

§ Department of Surgery, Osaka Medical Center for Cancer and Cardiovascular Diseases.

Published on Web 03/18/2009
10.1021/pr900092r CCC: $40.75

colorectal tissues revealed several inappropriate points as detailed below (data not shown): (1) GSLs contaminants from surrounding cells such as fibroblasts are often not negligible. (2) It takes a long time to extract cancer cells with high purity in sufficient amount for analysis (about 1 week for one tissue) and the technique is difficult to use in clinical applications. (3) It may be applicable in well or moderately differentiated adenocarcinomas which have a tubular structure making extraction of cancer cells relatively easy. However, it is impossible to extract cancer cells lying scattered about in cancerous tissues with high purity such as in poorly differentiated adenocarcinomas. Similarly, extraction of normal colorectal epithelial cells from normal colorectal tissues with high purity is also almost impossible due to the difficulty of separation of epithelial cells and lamina propria in colonic mucosa. To overcome these problems, we employ a method much superior to LMD in this study where colorectal cancer tissues and normal colorectal tissues were treated with collagenase, and colorectal cancer cells (CCs) and normal colorectal epithelial cells (NCs) isolated in high purity using the epithelial cell marker, CD326 and magnetic beads. Immunohistochemical studies using a monoclonal antibody that recognizes this epithelial cell marker revealed that CD326 is restricted to most normal epithelial cell types and cancer cells, but is not found on nonepithelial tissues and tumor cells from nonepithelial cells such as sarcoma and neurogenic tumors.[13] Magnetic beads labeled with antibody against CD326 have been used to isolate cancer cells from cancer tissues, peripheral blood and bone marrow.[14−16]

Other problems in previous analyses include that they are lacking in terms of identification and quantification due to the low sensitivity, low resolution, and poor quantification of conventional analytical methods such as thin layer chromatography and methylation analysis etc. These problems were solved in our previous study.[17] In this study we employed a powerful methodology to analyze the structures of GSLs which is applicable to small quantities of sample. The technique consists of release of the carbohydrate moieties of GSLs using endoglycoceramidase, fluorescent labeling with 2-aminopyridine and identification of each GSL by a two-dimensional (2-D) mapping technique together with tandem mass spectrometry. This highly sensitive, high resolution technique enabled us to identify 22 kinds of acidic GSLs including two novel fucogangliosides from 20 mg of colon cancer tissue from a liver metastasis lesion.

The final problem is that previous analyses were not comprehensive, with only a small number of samples from cancerous tissues analyzed. This might be due to the requirement of a number of techniques to determine the oligosaccharide structures, such as composition, sequence, linkage and anomericity of oligosaccharide moiety by conventional technique. Furthermore, most analyses have been performed using only cancer tissues, lacking normal tissue controls. Hence, variation of alteration of glycosylation in each patient has not been fully examined and the association of altered aberrant oligosaccharides with clinical data has not been proposed from the previous structural analyses. In contrast, structures of oligosaccharides are able to be ascertained with more alacrity using the method we employed than by conventional methods when we have enough standard oligosaccharides for the 2-D mapping technique, and the number of cases analyzed can be increased. Furthermore, as well as giving high purity cells, immuno-magnetic isolation of CCs and NCs helps to increase the number of cases analyzed, because the technique only takes a couple of hours and CCs and NCs can be prepared on the day of operation.

In this study, CCs and NCs were isolated from colorectal cancer tissues and normal colorectal mucosa from 16 colon cancer patients including 5 having liver metastasis and 1 lacking α1−4 fucosyltransferase, Lewis enzyme activity (This patient had liver metastasis). Using the advanced methods described above, structures of GSLs from these samples were analyzed. These precise and comprehensive analyses revealed general and varied structures of GSLs in NCs, and characteristic alterations of oligosaccharide structures in malignant transformation. Comparison of clinical data and the structures of GSLs in CCs showed a characteristic alteration in CCs from patients with liver metastasis and patients with high serum levels of CA19−9. Furthermore, we also examined the activities of related glycosyltransferses in NCs and CCs to understand the mechanism of generation of aberrant glycosylation.

Experimental Procedures

Standard PA-Oligosaccharides. Table 2 lists the structures, abbreviations and glucose units of all the pyridylaminated (PA) oligosaccharides reported in this study, which include PA-oligosaccharides commercially purchased, kindly donated, prepared from our previous study, and estimated in this study. Note two kinds of type 1-type 2 hybrid hexasaccharides, Galβ1−3GlcNAcβ1−3Galβ1−4GlcNAcβ1−3Galβ1−4Glc and Galβ1−4GlcNAcβ1−3Galβ1−3GlcNAcβ1−3Galβ1−4Glc are abbreviated as $_{2,1}Lc_6$ and $_{1,2}Lc_6$, respectively, in order of linkage type of the fourth and sixth galactose, in this paper.

Purification of Colorectal Cancer Cells and Normal Colorectal Epithelial Cells. All human specimens were obtained from Osaka Medical Center for Cancer and Cardiovascular Diseases and were processed for purification as described below. CCs and NCs were purified from primary lesions of colorectal cancers and their surrounding normal colorectal mucosa, respectively. The tissues were dissected into small blocks and incubated in DMEM/F12 medium containing 2 mg/mL collagenase (Sigma) for 60 min at 37 °C. Digested tissues were washed with PBS containing 10 mM EDTA, and filtered through 100 μm mesh. The cells were resuspended in PBS containing 2 mM EDTA and 0.5% BSA, and CD326 positive cells were positively selected using magnetically labeled microbeads (Milteny Biltec) according to the manufacture's protocol, snap frozen with liquid nitrogen, and stored at −80 °C until use. The number of CD326 positive cells obtained from cancerous and normal tissues was from 2×10^6 to 10^7, and the equal number of CCs and NCs were used to analyze (1×10^6). This study was approved by the Local Ethics Committee of Osaka Medical Center for Cancer and Cardiovascular Diseases. Informed consent was obtained from the patients.

Isolation of GSLs from CD326 Positive Colorectal Cancer Cells and Normal Colorectal Epithelial Cells. CD326 positive cells were extracted with 1200 μL of chloroform/methanol (2:1, v/v), followed by 800 μL of chloroform/methanol/water (1:2:0.8, v/v/v). Both extracts were loaded onto a DEAE-Sephadex A25 column, and flow though fractions collected as neutral GSLs and acidic GSLs eluted with 200 mM ammonium acetate in methanol. Acidic GSLs were desalted by gel filtration on a HW-40C column (TOSOH) equilibrated with chloroform/methanol/water (5:5:1, v/v/v). Neutral GSLs were dissolved in 50 μL of chloroform/methanol (2:1, v/v), 1 mL of acetone was added, and the sample stored at 4 °C overnight, and centri-

fuged. The pellets were incubated in 0.1 M NaOH in chloroform/methanol/water (5:5:1, v/v/v) at 37 °C for 1 h and desalted by gel filtration on a HW-40C column (TOSOH) equilibrated with chloroform/methanol/water (5:5:1, v/v/v).

Preparation of Pyridylaminated Oligosaccharides. The neutral and acidic GSLs were lyophilized and digested at 37 °C for 16 h with 10 mU of recombinant endoglycoceramidase II from *Rhodococcus* Sp. (Takara Bio Inc. Shiga, Japan) in 50 μL of 0.1 M sodium acetate (pH 5.0) containing 0.1% taurodeoxycholate.[18] Released oligosaccharides were labeled with 2-aminopyridine (2-AP).[19] Excess reagent in the reaction mixture with acidic GSLs was removed by cation exchange chromatograhy and phenol/chloroform extraction.[20] Neutral PA-oligosaccharides were purified by cation exchange chromatography followed by size fractionation HPLC.

High Performance Liquid Chromatography for PA-Oligosaccharide Separation. PA-oligosaccharides were separated on a Shimazu LC-20A HPLC system equipped with a Waters 2475 fluorescence detector. Normal phase HPLC was performed on a TSK gel Amide-80 column (0.2 × 25 cm, Tosoh) at 40 °C at a flow rate of 0.2 mL/min using two solvents, A and B. Solvent A was acetonitrile/0.5 M acetic acid containing 10% acetonitrile, adjusted to pH 7.3 with triethylamine (75:15, v/v). Solvent B was acetonitrile/0.5 M acetic acid containing 10% acetonitrile, adjusted to pH 7.3 with triethylamine (40:50, v/v). The column was equilibrated with solvent A. After injection of sample, the proportion of solvent B was programmed to increase from 0 to 100% in 100 min. The PA-oligosaccharides were detected by fluorescence with an excitation wavelength of 310 nm and an emission wavelength of 380 nm. The molecular size of each PA-oligosaccharide is given in glucose units (Gu) based on the elution times of PA-isomaltooligosaccharides. Reversed phase HPLC was performed on a TSK gel ODS-80Ts column (0.2 × 15 cm, Tosoh) at 30 °C at a flow rate of 0.2 mL/min using two solvents, C and D. Solvent C was 50 mM acetic acid, adjusted to pH 6.0 with triethylamine. Solvent D was 50 mM acetic acid containing 20% acetonitrile, adjusted to pH 6.0 with triethylamine. The column was equilibrated with solvent C. After injection of sample, the proportion of solvent D was programmed to increase from 0 to 18% in 54 min. The PA-oligosaccharides were detected by excitation at 315 nm and emission at 400 nm. The retention time of each PA-oligosaccharide is given in glucose units based on the elution times of PA-isomaltooligosaccharides. Thus, a given compound on these two columns provides a unique set of Gu (amide) and Gu (ODS) values, which correspond to coordinates of the 2-dimensional map (2-D map).

Electrospray Ionization MS^2. PA-oligosaccharides were analyzed by LC−ESI−MS/MS. High performance liquid chromatography was performed on a Paradigm MS4 equipped with a Magic C18 column (0.2 × 50 mm, Michrome BioResource, Auburn, CA). Each PA-oligosaccharide was injected with a flow rate of 2 μL/min for 3 min and eluted with 50% methanol for 10 min. MS analyses were performed using a LCQ ion trap mass spectrometer (Thermo Finnigan, San Jose, CA) equipped with a nanoelectrospray ion source (AMR, Tokyo, Japan). The nanospray voltage was set at 2.0 kV in the positive ion mode. The heated desolvation capillary temperature was set to 200 °C. In the LCQ method file, the LCQ was set to acquire a full MS scan between 400 and 2000 m/z followed by MS/MS scans in a data-dependent manner.

Sialyltransferase, Fucosyltransefarse and β-Galactosyltransferase Assays. CD326 positive cells were washed with phosphate-buffered saline and resuspended with 50 μL of 1% Triton X100 in 20 mM HEPES (pH 7.4), and subjected to sonication to obtain the cell homogenates. After centrifugation at 12 000 × g for 10 min, the supernatants were used as enzyme sources. The supernatants (1 μL) were assayed for sialyltransferase activities in 0.1 M cacodylate buffer, pH 6.5, 10 mM $MnCl_2$, 0.45% TritonX-100, 5 mM CMP-sialic acid (Sigma), and 1 mM PA-nLc_4 or PA-Lc_4 (a total volume of 5 μL). For fucosyltransefarse activities the assays were in 50 mM cacodylate buffer, pH 6.5, 5 mM ATP, 25 mM $MnCl_2$, 10 mM L-fucose, 75 μM GDP-fucose, and 1 mM PA-nLc_4 or PA-Lc_4 (a total volume of 5 μL). For β-galactosylltransferase activities the assays were in 20 mM HEPES buffer pH 7.4, 75 μM UDP-galactose, 10 mM $MnCl_2$, 0.01% Triton X-100 and 250 μM PA-Lc_3 (a total volume of 5 μL). Tetrasaccharides nLc_4 and Lc_4 were purchased from Sigma and pyridylaminated. PA-Lc_3 was prepared by releasing the terminal galactose of PA-Lc_4 with β-galactosidase from bovine testis (Sigma). The reaction mixtures for sialyltransferase activities using nLc_4 as acceptor, sialyltransferase activities using Lc_4 as acceptor, fucosyltransefarse activities, and β-galactosylltransferase activities were incubated at 37 °C for 30 min, 1 h, 2 h and 30 min, respectively. The reactions were terminated by boiling for 3 min. After centrifugation at 12 000 × g for 10 min, the supernatants were subjected to reverse phase HPLC for sialyltransferase activities, and size fractionation HPLC for fucosyltransefarse and β-galactosylltransferase activities, respectively. Enzyme activity is defined as picomoles of acceptor substrate sialylated, fucosylated or galactosylated per milligram of cell lysate protein per hour. The amounts of products were determined from their fluorescence intensities using pyridylaminated oligosaccharides as a standard. The reaction products were confirmed by 2-dimensional mapping and MS analysis.

Results

Preparation of PA-Oligosaccharides from CD326 Positive Colorectal Adenocarcinoma and Normal Colorectal Epithelial Cells. The clinicopathological features of the 16 patients examined in this study are summarized in Table 1. Of the 16 patients, 5 (cases 10−13, 16) suffered from hepatic metastasis, 2 (cases 14 and 15) showed very high serum levels of CA19−9, and 1 (case 16) lacked the activity of α1−4 fucosyltransferase, namely the Lewis enzyme, Fut III. CCs and NCs were purified from colorectal cancer tissues and surrounding normal colorectal tissues, respectively, utilizing epithelial cell marker CD326 and magnetic beads. The purity of these cells was confirmed to be nearly 100% as judged by immunocytochemical analysis using FITC-labeled CD326 antibody or microscopic observation of cytospinned cells stained with hematoxylin-eosin (Figure 1). Neutral and acidic GSLs were extracted from these cells. Glycans from the ceramide moieties were released by endoglycoceramidase II treatment, and the reducing ends of the released oligosaccharides were tagged with the fluorophore, 2-aminopyridine.

GSLs Identified in Colorectal Cancer and Normal Colorectal Epithelial Cells. The structures of acidic and neutral GSLs of CCs and NCs from 16 patients were analyzed in detail. A total of 300 peaks were collected from the first normal phase HPLC which were then separated into 408 peaks by a second

Table 1. Clinicopathological Information on the Patients with Colorectal Adenocarcinoma

no	age	sex	tumor localization	tumor size (mm)	histological differentiation	depth of invasion[a]	LN[a]	LM[a]	blood type	CEA (ng/mL)	CA19−9 (U/mL)
1	72	M	descending	33 × 30	well	SS	N1	H0	O	5.4	70
2	68	F	ascending	9 × 12	well	MP	N0	H0	O	13.3	0
3	67	M	sigmoid	40 × 85	well	SS	N1	H0	A	9.8	14
4	54	M	transverse	35 × 55	well	SS	N0	H0	A	0.8	2
5	79	M	ascending	33 × 45	moderately	SS	N0	H0	A	26.6	81
6	58	F	rectum	37 × 50	well	MP	N0	H0	A	0.9	6
7	55	F	ascending	28 × 80	well	SS	N0	H0	O	1.3	22
8	71	M	ascending	25 × 25	moderately	SE	N1	H0	O	8.8	27
9	64	M	ascending	34 × 34	moderately	SS	N2	H0	O	4.2	11
10	82	M	cecum	25 × 56	well	SS	N0	H1	O	2.2	12
11	47	F	sigmoid	55 × 74	well > moderately	SS	N0	H1	O	9.8	8
12	59	F	ascending	50 × 55	poorly > moderately	SS	N1	H1	O	3.8	11
13	71	F	sigmoid	31 × 30	well	SS	N1	H1	B	10.8	16
14	74	M	rectum	30 × 30	well	A (1mm)	N1	H0	AB	12.8	344
15	69	M	rectosigmoid	49 × 65	poorly	SS	N1	H0	A	2.2	157
16	58	F	rectum	55 × 50	moderately	SE	N3	H2	O	27.0	0

[a] LN, lymph node metastasis; LM, liver metastasis; SS, subserosa; MP, muscularis propria; SE, serosa exposed; A, adventitia; Si, invasion to neighboring tissue.

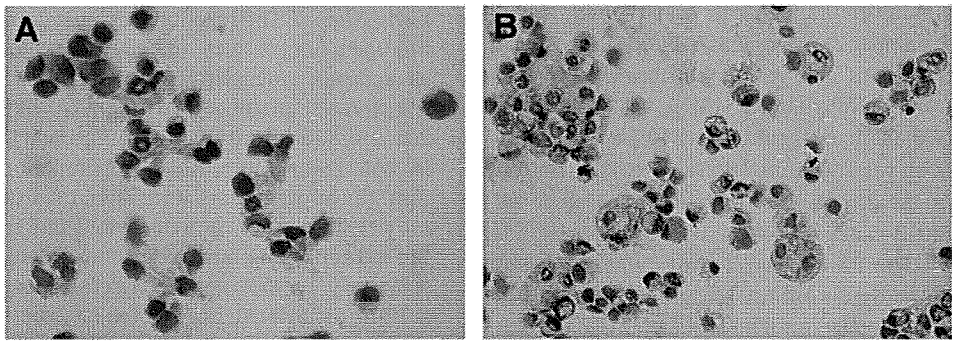

Figure 1. CD326 positive cells isolated from colorectal cancer tissues (A) and normal colorectal tissues (B) H&E staining.

reverse phase HPLC run. All the peaks were subjected to mass spectrometry analysis. From comparison of the positions on the map with the standards we purchased and have already acquired from our previous study together with subsequent mass spectrometry analysis, the structures of most of the PA-oligosaccharides could be estimated. We identified 27 and 28 kinds of acidic and neutral GSLs, respectively, from CCs and NCs of the 16 patients. The structures, abbreviations and elution positions of these species are listed in Table 2. Among them, 9 kinds of oligosaccharides, A11−2, A12−3, A14, A16−2, N12, N16, N17−1, N19, N22 did not match to the acquired standards and are estimated in this study using enzymatic digestion with α-*N*-acetylgalactosaminidase, α1,3/4-fucosidase, and α1,2-fucosidase (data not shown).

Comparison of the Structures of GSLs of Colorectal Cancer Cells and Normal Colorectal Epithelial Cells from a Representative Case. To investigate the alteration of structures of GSLs of CCs in carcinogenesis, the structures of GSLs of CCs and NCs from 16 patients were precisely analyzed and carefully compared. No significant difference of total quantities of PA-oligosaccharides obtained from CCs and NCs were found. The estimated structures of PA-oligosaccharides from CCs and NCs from 16 patients are summarized in Supplementary Table 1 (Supporting Information). However, in this results section, the chromatograms from the first normal phase HPLC are shown, because most peaks are composed of one PA-oligosaccharide, are easy to understand and allow easy comparison of the profiles of oligosaccharide. When the peaks are composed of two or more kinds of PA-oligosaccharide, the ratios of the oligosaccharide are made clear in each case.

Most of the NCs, with a few exceptions, exhibit similar GSL structures. Furthermore, we found three characteristic changes in the structures of GSLs in carcinogenesis. Hence, we show representative structures of CCs and NCs initially in Figure 2. Figure 2B and 2D show the profiling of acidic and neutral GSLs of NCs from case 1. The highest peak N9 of the neutral GSLs is a mixture of Le^a (N9−2) and Le^x (N9−1). These two are the only PA-oligosassacrides in our standard oligosaccharides which have almost the same elution position in both types of HPLC (ODS and amide), and cannot be separated even on the second reverse phase HPLC run. Hence, the ratio of Le^a (N9−2) and Le^x (N9−1) in peak N9 was determined by converting the mixture to Lc_4 and nLc_4 by α1/3.4 fucosidase digestion followed by separation by reverse phase HPLC. The chromatogram is shown inset beside peak N9. Peak N24 is also a mixture of two difucosylated oligosaccharides, ending in type-2 and type-1 lactosamine chains, V^3FucαIII^{3}Fucα-nLc_6 (N24−1) and V^4Fucα-III^{3}Fucα-$_{2,1}Lc_6$ (N24−2), respectively, which can be separated by the second RP HPLC run. The chromatogram is shown inset beside peak 24. As shown in Figure 2B and D, it is easily seen by comparison of the profiles of neutral and acidic GSLs that neutral GSLs are the major products in NCs. The dominant peak of the neutral GSLs in NCs is N9, which is composed of mainly type-1 chain, Le^a (N9−2) with type-2 chain, Le^x (N9−1) being a very minor constituent (97% Le^a, 3% Le^x, in this case). Furthermore, significant amounts of lactose(N1), Le^b(N13),

Table 2. Assigned Structures of PA-Oligosaccharides from Colorectal Cancer Cells and/or Normal Colorectal Epithelial Cells

Fraction	Structure	Abbreviation	NP	RP
Acidic				
A1	HSO_3-3Galβ1-4Glc-PA	SM3	1.19	2.60
A2	Neu5Acα2-3Galβ1-4Glc-PA	GM3	2.46	3.00
A3	GalNAcβ1-4Galβ1-4Glc-PA 3 Neu5Acα2	GM2	2.97	3.01
A4	Neu5Acα2-8Neu5Acα2-3Galβ1-4Glc-PA	GD3	3.31	4.50
A5	GalNAcβ1-4Galβ1-4Glc-PA 3 Neu5Acα2-8Neu5Acα2	GD2	3.78	4.23
A6	Galβ1-3GalNAcβ1-4Galβ1-4Glc-PA 3 Neu5Acα2	GM1	3.85	2.92
A7-1	Neu5Acα2-3Galβ1-4GlcNAcβ1-3Galβ1-4Glc-PA	SPG	4.02	4.52
A7-2	Neu5Acα2-3Galβ1-3GlcNAcβ1-3Galβ1-4Glc-PA	LST-a	4.01	4.69
A8	Galβ1-3GalNAcβ1-4Galβ1-4Glc-PA 3 3 Neu5Acα2 Neu5Acα2	GD1a	4.10	5.03
A9	Galβ1-3GlcNAcβ1-3Galβ1-4Glc-PA 6 Neu5Acα2	LST-b	4.18	3.10
A10	Neu5Acα2-6Galβ1-4GlcNAcβ1-3Galβ1-4Glc-PA	LST-c	4.40	3.76
A11-1	Galβ1-3GalNAcβ1-4Galβ1-4Glc-PA 3 Neu5Acα2-8Neu5Acα2	GD1b	4.64	3.96
A11-2	Neu5Acα2 6 Galβ1-3GlcNAcβ1-3Galβ1-4Glc-PA 4 Fucα1	$III^6NeuAc\alpha III^4Fuc\alpha$-$Lc_4$	4.65	2.92
A12-1	Neu5Acα2-3Galβ1-4GlcNAcβ1-3Galβ1-4Glc-PA 3 Fucα1	SLe^x	4.75	4.08
A12-2	Neu5Acα2-6Galβ1-4GlcNAcβ1-3Galβ1-4Glc-PA 2 Fucα1	$IV^2Fuc\alpha IV^6NeuAc\alpha$-$nLc_4$	4.74	5.35
A12-3	Neu5Acα2-3Galβ1-3GlcNAcβ1-3Galβ1-4Glc-PA 6 Neu5Acα2	$IV^3NeuAc\alpha III^6NeuAc\alpha$-$Lc_4$	4.52	5.54
A13-1	Neu5Acα2-3Galβ1-3GlcNAcβ1-3Galβ1-4Glc-PA 4 Fucα1	SLe^a	4.92	3.77
A13-2	Galβ1 -3GalNAcβ1 -4Galβ1 -4Glc-PA 3 3 Neu5Acα2 Neu5Acα2-8Neu5Acα2	GT1b	4.85	6.34
A14	Neu5Acα2 6 Neu5Acα2-3Galβ1-3GlcNAcβ1-3Galβ1-4Glc-PA 4 Fucα1	$IV^3NeuAc\alpha III^6NeuAc\alpha III^4Fuc\alpha$-$Lc_4$	5.05	5.15
A15	Neu5Acα2-3Galβ1-4GlcNAcβ1-3Galβ1-4GlcNAcβ1-3Galβ1-4Glc-PA	$VI^3NeuAc\alpha$-nLc_6	5.51	5.64

Table 2. Continued

Fraction	Structure	Abbreviation	NP	RP
A16-1	Neu5Acα2-6Galβ1-4GlcNAcβ1-3Galβ1-4GlcNAcβ1-3Galβ1-4Glc-PA	VI^6NeuAcα-nLc$_6$	5.89	4.71
A16-2	Neu5Acα2-6Galβ1-4GlcNAcβ1-3Galβ1-3GlcNAcβ1-3Galβ1-4Glc-PA	VI^6NeuAcα-$_{1,2}$Lc$_6$	5.77	5.45
A17	Neu5Acα2-6Galβ1-4GlcNAcβ1-3Galβ1-4GlcNAcβ1-3Galβ1-4Glc-PA 2 | Fucα1	VI^2FucαVI^{6}NeuAcα-nLc$_6$	6.17	5.82
A18	Neu5Acα2-6Galβ1-4GlcNAcβ1-3Galβ1-4GlcNAcβ1-3Galβ1-4Glc-PA 3 | Fucα1	VI^6NeuAcαIII^{3}Fucα-nLc$_6$	6.71	4.19
A19	Neu5Acα2-3Galβ1-4GlcNAcβ1-3Galβ1-4GlcNAcβ1-3Galβ1-4GlcNAcβ1-3Galβ1-4Glc-PA	VIII^{3}NeuAcα-nLc$_8$	6.85	6.78
A20-1	Neu5Acα2-3Galβ1-4GlcNAcβ1-3Galβ1-4GlcNAcβ1-3Galβ1-4Glc-PA 3 3 | | Fucα1 Fucα1	VI^3NeuAcαV^{3}FucαIII^{3}Fucα-nLc$_6$	7.04	4.16
A20-2	Neu5Acα2-6Galβ1-4GlcNAcβ1-3Galβ1-4GlcNAcβ1-3Galβ1-4Glc-PA 2 3 | | Fucα1 Fucα1	VI^2FucαVI^{6}NeuAcαIII^{3}Fucα-nLc$_6$	7.00	5.04
Neutral				
N1	Galβ1-4Glc-PA	lactose	2.03	0.93
N2	GlcNAcβ1-3Galβ1-4Glc-PA	Lc$_3$	2.76	2.11
N3	Galα1-4Galβ1-4Glc-PA	Gb$_3$	2.84	1.06
N4	GalNAcβ1-3Galα1-4Galβ1-4Glc-PA	Gb$_4$	3.47	2.71
N5	Galβ1-3GlcNAcβ1-3Galβ1-4Glc-PA	Lc$_4$	3.66	2.50
N6	Galβ1-4GlcNAcβ1-3Galβ1-4Glc-PA	nLc$_4$	3.74	2.16
N7	Fucα1-2Galβ1-4GlcNAcβ1-3Galβ1-4Glc-PA	type II H	4.15	3.80
N8	Fucα1-2Galβ1-3GlcNAcβ1-3Galβ1-4Glc-PA	type I H	4.23	2.86
N9-1	Galβ1-4GlcNAcβ1-3Galβ1-4Glc-PA 3 | Fucα1	Le^x	4.51	1.99
N9-2	Galβ1-3GlcNAcβ1-3Galβ1-4Glc-PA 4 | Fucα1	Le^a	4.51	2.01
N10	GalNAcα1-3Galβ1-3GlcNAcβ1-3Galβ1-4Glc-PA 2 | Fucα1	Type I A	4.67	3.89
N11	Fucα1-2Galβ1-4GlcNAcβ1-3Galβ1-4Glc-PA 3 | Fucα1	Le^y	4.98	2.96
N12	Galβ1-3GlcNAcβ1-3Galβ1-3GlcNAcβ1-3Galβ1-4Glc-PA	Lc$_6$	5.13	3.58
N13	Fucα1-2Galβ1-3GlcNAcβ1-3Galβ1-4Glc-PA 4 | Fucα1	Le^b	5.21	1.42
N14	GlcNAcβ1-3Galβ1-4GlcNAcβ1-3Galβ1-4Glc-PA 3 | Fucα1	agalacto III^{3}Fucα-nLc$_6$	5.20	2.49
N15	Galβ1-4GlcNAcβ1-3Galβ1-4GlcNAcβ1-3Galβ1-4Glc-PA	nLc$_6$	5.38	2.93
N16	GalNAcα1-3Galβ1-4GlcNAcβ1-3Galβ1-4Glc-PA 2 3 | | Fucα1 Fucα1	ALe^y	5.63	1.45

Table 2. Continued

Fraction	Structure	Abbreviation	NP	RP
N17-1	Galβ1-3GlcNAcβ1-3Galβ1-3GlcNAcβ1-3Galβ1-4Glc-PA 2 | Fucα1	VI^{2}Fucα-Lc$_6$	5.66	3.78
N17-2	Galβ1-4GlcNAcβ1-3Galβ1-4GlcNAcβ1-3Galβ1-4Glc-PA 2 | Fucα1	VI^{2}Fucα-nLc$_6$	5.77	4.13
N18	GalNAcα1-3Galβ1-3GlcNAcβ1-3Galβ1-4Glc-PA 2 4 | | Fucα1 Fucα1	ALe^b	5.73	1.91
N19	Galβ1-4GlcNAcβ1-3Galβ1-3GlcNAcβ1-3Galβ1-4Glc-PA 3 | Fucα1	V^{3}Fucα-$_{1,2}$Lc$_6$	6.03	2.96
N20-1	Galβ1-4GlcNAcβ1-3Galβ1-4GlcNAcβ1-3Galβ1-4Glc-PA 3 | Fucα1	V^{3}Fucα-nLc$_6$	6.12	2.49
N20-2	Galβ1-3GlcNAcβ1-3Galβ1-4GlcNAcβ1-3Galβ1-4Glc-PA 3 | Fucα1	III^{3}Fucα-$_{2,1}$Lc$_6$	6.12	2.70
N21	Galβ1-4GlcNAcβ1-3Galβ1-4GlcNAcβ1-3Galβ1-4Glc-PA 3 | Fucα1	III^{3}Fucα-nLc$_6$	6.23	2.51
N22	Galβ1-4GlcNAcβ1-3Galβ1-4GlcNAcβ1-3Galβ1-4Glc-PA 2 3 | | Fucα1 Fucα1	VI^{2}FucαV^{3}Fucα-nLc$_6$	6.63	3.10
N23	Galβ1-4GlcNAcβ1-3Galβ1-4GlcNAcβ1-3Galβ1-4GlcNAcβ1-3Galβ1-4Glc-PA	nLc$_8$	6.88	4.20
N24-1	Galβ1-4GlcNAcβ1-3Galβ1-4GlcNAcβ1-3Galβ1-4Glc-PA 3 3 | | Fucα1 Fucα1	V^{3}FucαIII^{3}Fucα-nLc$_6$	6.99	2.14
N24-2	Galβ1-3GlcNAcβ1-3Galβ1-4GlcNAcβ1-3Galβ1-4Glc-PA 4 3 | | Fucα1 Fucα1	V^{4}FucαIII^{3}Fucα-$_{2,1}$Lc$_6$	7.05	2.37

V^{3}FucαIII^{3}Fucα-nLc$_6$(N24−1) and V^{4}FucαIII^{3}Fucα-$_{2,1}$Lc$_6$(N24−2) are found. It is noteworthy that in NCs, in a way similar to the relationship between Le^a (N9−2) and Le^x (N9−1) in peak N9, the expression level of V^{4}FucαIII^{3}Fucα-$_{2,1}$Lc$_6$(N24−2), terminating in the type-1 lactosamine chain, is more than that of V^{3}FucαIII^{3}Fucα-nLc$_6$ (N24−1), terminating in the type-2 lactosamine chain (75% V^{4}FucαIII^{3}Fucα-$_{2,1}$Lc$_6$, 25% VI^{3}Fucα,III^{3}Fucα-nLc$_6$, in this case). In addition, globo-series Gb$_3$(N3) and Gb$_4$(N4), and a small amount of Lc$_4$(N5) and nLc$_4$(N6) are observed. The amount of acidic GSLs in NCs is much lower than that of neutral GSLs, which include very small amounts of SM3(A1), ganglio-series GM3 (A2), GD3 (A4), GM1 (A6), and GD1a(A8), and neolacto-series LST-c(A10). The profile of GSLs from NCs is very similar in most cases with the few exceptions. The structures of acidic and neutral GSLs from CCs from this case are shown in Figure 2A and 2C, respectively. Alterations in the structures of GSLs of CCs in carcinogenesis occurred in most of the cases analyzed in this study can be summarized as involving increases of three kinds: (1) the ratio of type-2 chain oligosaccharides, (2) α2−6 and/or α2−3 sialylation, and (3) α1−2 fucosylation. In the elevation of the ratio of type-2 chains, the ratio of Le^x (N9−1) in N9, the main peak in neutral GSLs in CCs, is elevated compared to that of in N9 from NCs (see insets of N9 Figure 2C and D). Similarly, the ratio of V^{3}FucαIII^{3}Fucα-nLc$_6$(N24−1) and V^{4}FucαIII^{3}Fucα-$_{2,1}$Lc$_6$(N24−2) in peak N24 were reversed in carcinogenesis in most cases. Thus, the expression level of V^{3}FucαIII^{3}Fucα-nLc$_6$(N24−1), which is less abundant than V^{4}FucαIII^{3}Fucα-$_{2,1}$Lc$_6$ (N24−2) in NCs, was higher than V^{4}FucαIII^{3}Fucα-$_{2,1}$Lc$_6$(N24−2) in CCs (see insets of N24, Figure 2C and D). In addition, type-2 chain nLc$_4$(N6), which is undetected or at a negligible level in NCs, is significantly elevated in CCs. With sialylation, although significant alteration of the levels of the ganglio-series GSLs was not found, sialylated neolacto- and lacto-series GSLs were significantly increased in carcinogenesis. The main peak LST-c (A10), terminal α2−6 sialylated nLc$_4$, is markedly increased in carcinogenesis. Similarly, α2−6 sialylated III^{3}Fucα-nLc$_6$ (A18), which is not detected in NCs from most cases, is significantly expressed in CCs. With regard to α2−3 sialylation, SLe^a (A13−1), which is not usually detected in NCs, is found in CCs. In the acidic fraction in CCs, besides the above three acidic GSLs, SLe^x(A12−1), IV^{2}FucαIV^{6}NeuAcα-

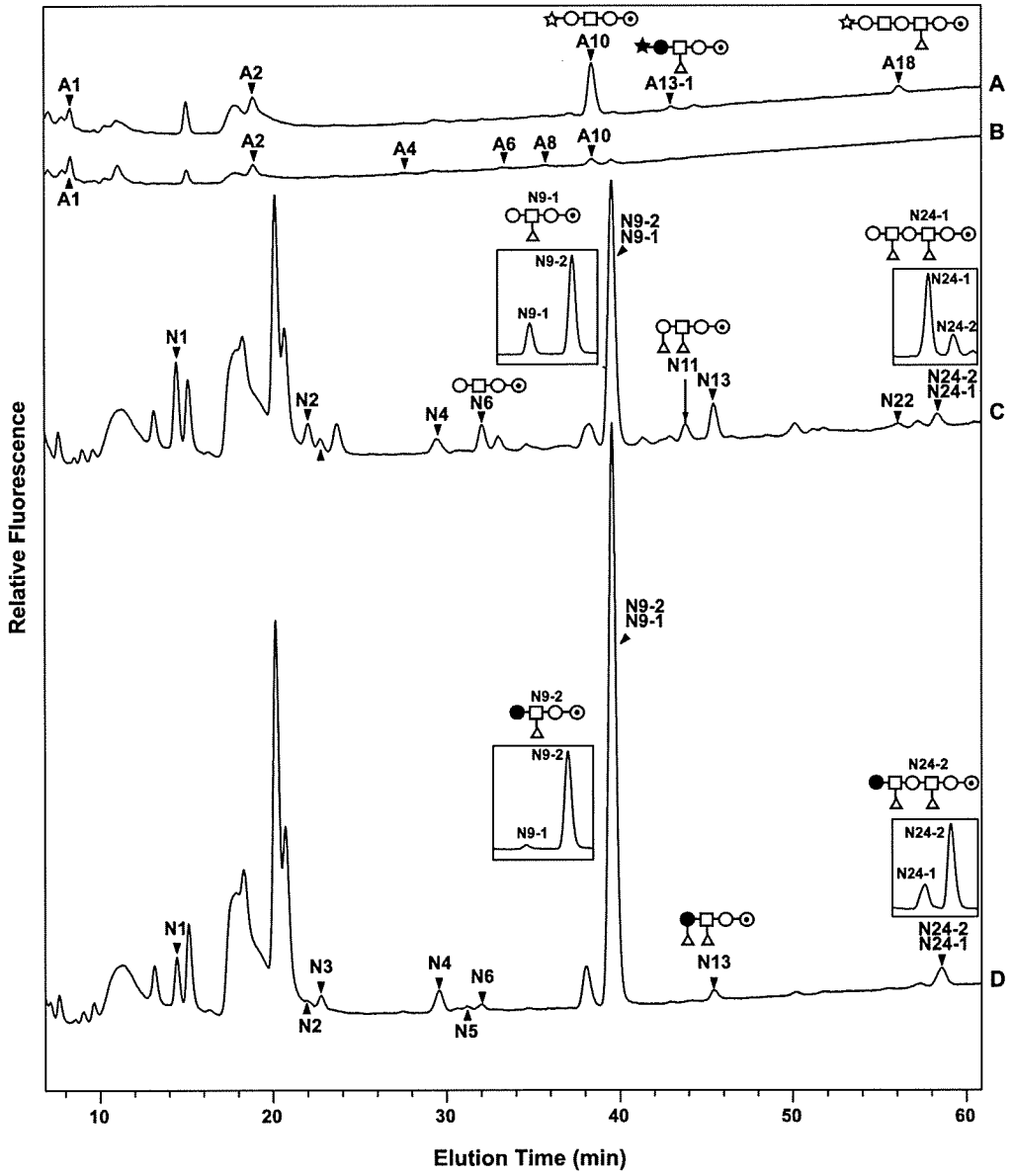

Figure 2. Comparison of amide column HPLC profiles of acidic and neutral PA-oligosaccharides obtained from CCs and NCs from a representative case (case 1). (A) Acidic fraction of CCs, (B) acidic fraction of NCs, (C) neutral fraction of CCs, (D) neutral fraction of NCs. Identified PA oligosaccharides in each peak are highlighted with closed arrowheads and numbered with fraction numbers as per Table 2. Peak N9 and N24 are mixtures of Le^a (N9−2) and Le^x (N9−1), and $V^3Fuc\alpha III^3Fuc\alpha$-$nLc_6$(N24−1), and $V^4Fuc\alpha III^3Fuc\alpha$-$_{2,1}Lc_6$(N24−2), respectively. The ratio of Le^a (N9−2) and Le^x (N9−1) in peak N9 was determined by α1,3/4-fucosidase digestion followed by reverse phase HPLC, and the chromatogram is shown inset besides peak N9. The ratio of $V^3Fuc\alpha III^3Fuc\alpha$-$nLc_6$(N24−1) and $V^4Fuc\alpha III^3Fuc\alpha$-$_{2,1}Lc_6$(N24−2) in peak N24 was determined by reverse phase HPLC, and the chromatogram is shown inset besides peak N24. Schemes of representative oligosaccharides are shown. Symbols; open circle with a dot inside: glucose, open circle: galactose (β1−4 linkage, type 2), closed circle: galactose (β1−3 linkage, type 1), open square: GlcNAc, open star: sialic acid (α2−6 linkage), closed star: sialic acid (α2−3 linkage), open triangle: fucose.

nLc_4(A12−2) and $VI^3NeuAc\alpha$-nLc_6(A15) were often found but are not found in NCs in other cases (case 4, 6, 9, 10, 11, 14, 16). With respect to α1−2 fucosylation, Le^b (N13) is elevated, and Le^y(N11) appears/is elevated in carcinogenesis, probably accompanied by the elevation of the type-2 chain oligosaccharide, nLc_4. Only Le^y(N11) and Le^b(N13) were observed as α1−2 fucosylated products in the neutral fractions in CCs from most cases. However, in addition to Le^y(N11) and Le^b(N13), high expression of other α1−2 fucosylated products, including $IV^2Fuc\alpha$-nLc_4(N7, type II H), $IV^2Fuc\alpha$-Lc_4(N8, type I H), $VI^2Fuc\alpha$-nLc_6 (N17−2) and $VI^2Fuc\alpha V^3Fuc\alpha$-$nLc_6$ (N22) were found in CCs from 3 patients, cases 7, 12, and 16.

Alteration of the Ratio of Type-2 Oligosaccharides, Sialylation and α1−2 Fucosylation in Malignant Transformation of Colorectal Cancers. Since the degree of the three kinds of alteration is fairly different case by case, the ratio of type-2 oligosaccharides, sialylation and α1−2 fucosylation of CCs and NCs from all 16 cases are shown in Figure 3. The ratio of type-2 chain oligosaccharides is defined as the amount of Le^x (N9−1)

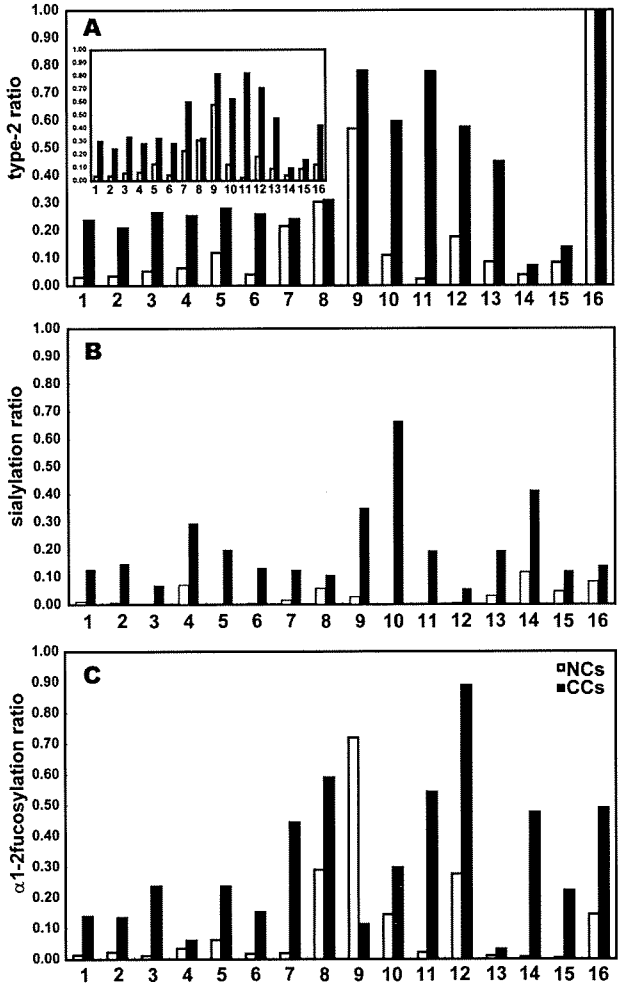

Figure 3. Comparison of the ratio of type-2, sialylated, and α1−2 fucosylated PA-oligosaccharides obtained from CCs and NCs. (A) Ratio of type-2 oligosaccharides. The ratio of Le^x and Le^y/total amount of Le^a, Le^b, Le^x and Le^y of CCs and NCs is shown. (Inset) Ratio of the total amount of nLc_4 and fucosylated derivatives of nLc_4/the total amount of nLc_4 and Lc_4 and their fucosylated derivatives. (B) Ratio of sialylated oligosaccharides. The ratio of total amounts of α2−3 and/or α2−6 sialylated neolacto or lacto series oligosaccharides/neolacto or lacto series oligosaccharides of CCs and NCs is shown. (C) Ratio of α1−2 fucosylated oligosaccharides. The ratio of total amounts of α1−2 fucosylated neolacto or lacto series GSLs/neolacto or lacto series neutral GSLs of CCs and NCs is shown. Open and filled bars indicate NCs and CCs, respectively.

plus Le^y(N11)/ total amount of Le^a(N9−2), Le^b(N13), Le^x (N9−1) and Le^y(N11), because these 4 kinds of oligosaccharides are dominant products of type-1 and type-2 in both CCs and NCs of most cases. The ratios of type-2 are increased in malignant transformation in all cases with one exception, case 16 (Figure 3A). Case 16 lacks the Lewis enzyme activity which results in defect of Le^a(N9−2) and Le^b(N13), and the type-2 ratio defined as above is understandably 1. Even though the type-2 ratio is defined as the total amount of nLc_4 and fucosylated derivatives of nLc_4/the total amount of nLc_4 and Lc_4 and their fucosylated derivatives, the type-2 ratio from most cases are not significantly altered, with the exception of case 7 and case 16 (Figure 3A inside).

The ratio of sialylation is defined as the total amount of α2−3 and/or α2−6 sialylated neolacto or lacto series GSLs/neolacto or lacto series GSLs and the ratios are shown in Figure 3B. Sialylation is increased in malignant transformation without exception.

The ratio of α1−2 fucosylation is defined as the total amount of α1−2 fucosylated neolacto or lacto series GSLs/neolacto or lacto series neutral GSLs and the ratios are shown in Figure 3C. The elevations in the ratio of type-2 chain and sialylation were found in all cases in carcinogenesis of CCs. Similarly, α1−2 fucosylation is increased in CCs from most cases although we found 1 exception, case 9.

Structures of GSLs from CCs and NCs in Cases Where Type-2 Chain Oligosaccharides Dominate in CCs. As shown in Figure 3A, the type-2 ratios of the NCs are around or lower than 10%, and increased to around 20 − 30% in carcinogenesis in most cases. Thus, type-2 oligosaccharides are still minor products in CCs from most cases. However, we found 6 cases exhibiting a type-2 ratio of around 50% or more in CCs. Five of these cases (case 10, 11, 12, 13 and 16) resulted from the marked elevation of type-2 species which are very minor in NCs, and 1 case (case 9) resulted from a slight increase of type-2 species which are major components of the GSLs of NCs. The common clinical feature of the former 5 cases (cases 10, 11, 12, 13 and 16) is the presence of hepatic metastasis (Table 1). Figure 4 shows the profiling of GSLs from NCs and CCs of case 11. The structures of GSLs from NCs are mainly composed of type-1 chains, similar to the representative case described above (Figure 4D), with Le^a(N9−2), dominating peak N9, and lactose(N1) being major products, and Le^b(N13) being a minor product (Figure 4D). In peak N24, only $V^4FucαIII^3Fucα\text{-}_{2,1}Lc_6$(N24−2) (but no $V^3FucαIII^3Fucα\text{-}nLc_6$(N24−1)) is found. Expression of acidic GSLs is very low (Figure 4B). In carcinogenesis in this case, a shift from type-1 dominant to type-2 dominant was found in neutral GSLs; peak N9 was converted to mainly Le^x (N9−1) from Le^a (N9−2), peak Le^y (N11) is higher than Le^b (N13), $V^4FucαIII^3Fucα\text{-}_{2,1}Lc_6$(N24−2) disappeared, only $V^3FucαIII^3Fucα\text{-}nLc_6$ (N24−1) is found in peak 24, and nLc_4(N6) was observed as the main peak (Figure 4C). However, elevation of Le^y is not common in the 5 cases, and such elevation was not found in the CCs from two of the cases (cases 10 and 13) In the acidic fraction, in addition to the peaks shown in the representative case, (LST-c (A10) and $VI^6NeuAcαIII^3Fucα\text{-}nLc_6$ (A18)), $VI^3NeuAcα\text{-}nLc_6$(A15) was observed and peak A12, a mixture of SLe^x(A12−1) and $IV^2FucαIV^6NeuAcα\text{-}nLc4$(A12−2) reached a level higher than or equivalent to SLe^a (A13−1), probably accompanied by an increase in their precursor, type-2 nLc_4(N6). The level of SLe^x(A12−1) and $IV^2FucαIV^6NeuAcα\text{-}nLc_4$(A12−2) is almost equivalent in this case.

Structures of GSLs of CCs and NCs from the Cases Specifically Demonstrating Elevation of α2−3 Sialylation in Carcinogenesis. In the elevation of sialylation in carcinogenesis usually observed in this study, elevation of α2−6 is more pronounced than that of α2−3 (the small quantity of LSTc in NCs is increased such that it becomes the main product in the acidic fraction in carcinogenesis). In contrast, sialylated derivatives of Lc_4, such as SLe^a(A13−1), $IV^3NeuAcαIII^6NeuAcα\text{-}Lc4$(A12−3) and $IV^3NeuAcαIII^6NeuAcαIII^4Fucα\text{-}Lc4$(A14) are not detected in most NCs, and they still appear as very minor peaks in the acidic fraction in CCs from most cases. However, we found 2 cases (cases 14 and 15) in which α2−3 sialylation to type-1 chain is much preferred to α2−6 sialylation to type-2 chain in carcinogenesis. Profiling of the acidic and neutral GSLs of CCs and NCs from case 15 is shown in Figure 5. The profile of neutral GSLs of NCs is similar to that generally observed

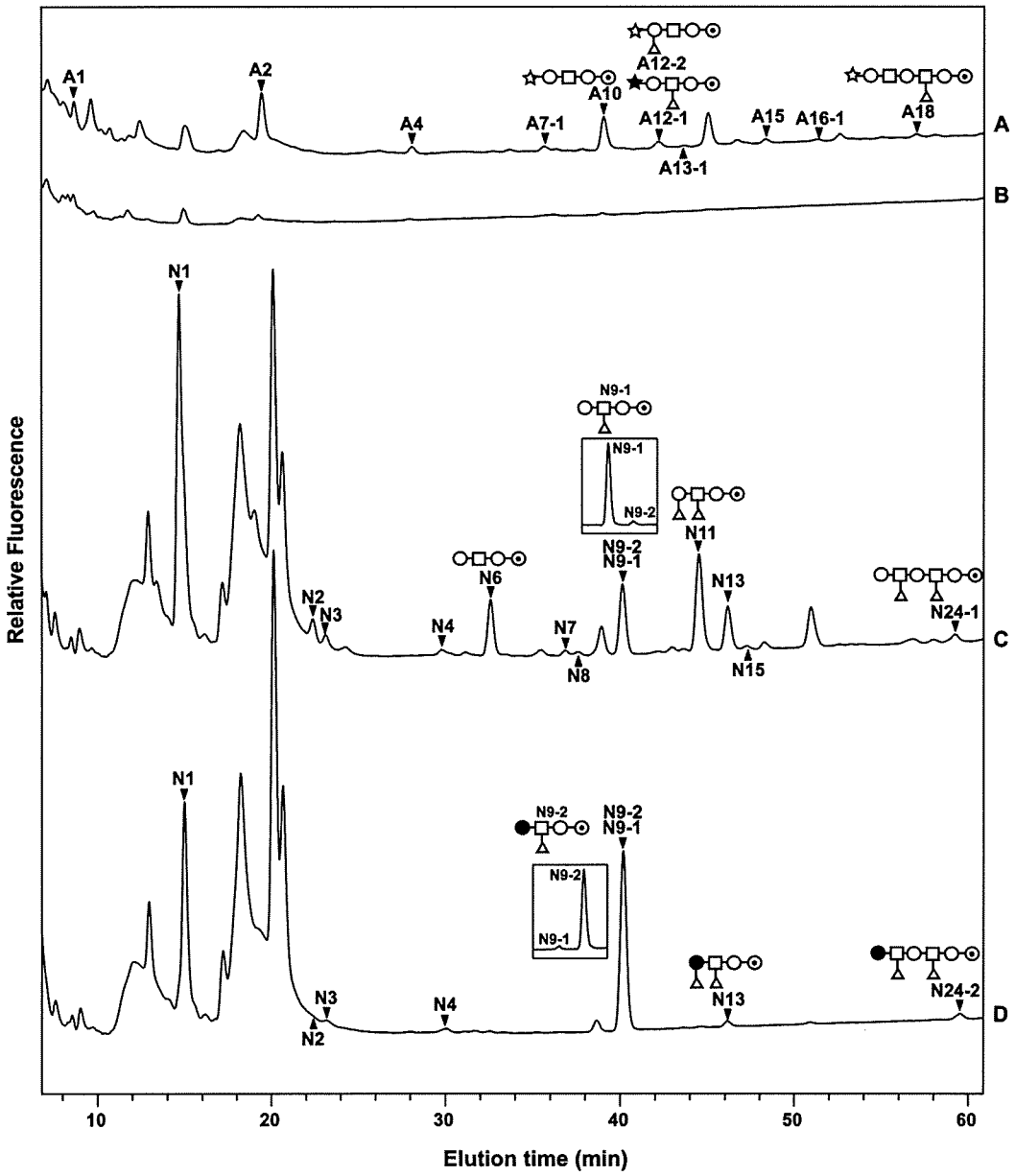

Figure 4. Comparison of amide column HPLC profiles of acidic and neutral PA-oligosaccharide obtained from CCs and NCs from case 11. The shift from type-1 dominant to type-2 dominant in malignant transformation is observed. A, acidic fraction of CCs, B, acidic fraction of NCs, C, neutral fraction of CCs, D, neutral fraction of NCs. Identified PA-oligosaccharides of each peak, the ratio of mixtures of peak N9 and schemes are shown as in Figure 2.

(Figure 5D). In contrast, the profile of the acidic fraction is slightly different to that generally observed (Figure 5B) in terms of the presence of α2−3 sialylated derivatives in addition to α2−6 sialylated nLc_4, LST-c (A10), which are usually found in NCs. α2−3 sialylated derivatives of nLc_4, SPG (A7−1) and SLe^x (A12−1), and α2−3 sialylated derivatives of Lc_4, SLe^a (A13−1) and $IV^3NeuAc\alpha III^6NeuAc\alpha III^4Fuc\alpha$-$Lc_4$ (A14), were found in the acidic fraction of NCs even though their expression levels were very low. This is noteworthy as they are usually below detection limits in normal NCs (Figure 5B). In carcinogenesis in these two cases, elevation of the ratio of type-2 chain is minimal; Le^a (N9−2) is dominant in peak N9, and Le^b (N13) is much higher than Le^y (N11) (Figure 5C). Elevation of α1−2 fucosylation occurred, and increased Le^b(N13) and ALe^b(N18) were found. One of the most characteristic features of the two cases is that high and specific elevation of α2−3 sialylation on type-1 chain occurred, in particular, SLe^a (A13−1) became the major peak in CCs. In contrast, LST-c (A10), usually elevated in carcinogenesis, is decreased in this case, and not altered in CCs of case 14. The common feature of the 2 cases is a very high serum level of CA19−9 (Table 1).

Structures of GSLs of CCs and NCs from a Patient Lacking Lewis Enzyme Activity. One case (case 16) out of the 16 lacked the activity of α1−4 fucosyltransferase, the Lewis enzyme, Fut III. This patient had liver metastasis. Figure 6 shows the profiling of GSLs from CCs and NCs from this case. Peak N9 and N24 from NCs and CCs, which are composed of mixtures of Le^a (N9−2) and Le^x (N9−1), and $V^4Fuc\alpha III^3Fuc\alpha$-$_{2,1}Lc_6$(N24−2) and $V^3Fuc\alpha III^3Fuc\alpha$-$nLc_6$ (N24−1), respectively, when the subjects have sufficient activity of α1−4 fucosyltransferase, in this case are composed of only Le^x (N9−1) and $V^3Fuc\alpha III^3Fuc\alpha$-$nLc_6$ (N24−1), respectively (Figure 6C and D). However, instead of Le^a, Lc_4 (N5) and α1−2 fucosylated Lc_4 (N8) are observed to be the major products in NCs (Figure 6D). In